Cytokine-regulated neutrophil recruitment is required for brain but not spinal cord inflammation during EAE

Sarah B. Simmons

A dissertation submitted in partial fulfillment of the requirements for the degree of

Doctor of Philosophy

University of Washington

2014

Committee:

Joan Goverman

Denny Liggitt

Estelle Bettelli

Jonathan Weinstein

Keith Elkon

Program Authorized to Offer Degree:

Immunology

University of Washington

Abstract

IL-17 and IFN-γ regulate neuroinflammatory patterns by differentially influencing neutrophil recruitment in the brain versus the spinal cord

Sarah Beth Simmons

Chair of the Supervisory Committee:

Joan Goverman, Ph.D.

Department of Immunology

Multiple sclerosis is an autoimmune disease characterized by inflammatory lesions throughout the central nervous system (CNS). The location of lesions is a critical determinant of clinical signs but varies among patients. While both IFN-γ and IL-17 signaling influence lesion location in mouse models of MS, the mechanisms underlying their activities are unknown. We show that IL-17 promotes, but IFN-γ inhibits, ELR+ chemokine-mediated neutrophil recruitment to the brain, which is required for parenchymal tissue damage in the brain. In contrast, IFN-γ promotes rather than inhibits ELR+ chemokine expression and neutrophil recruitment in the spinal cord. Surprisingly, tissue injury in the spinal cord does not exhibit the same dependence on neutrophils that was observed for the brain. Thus, the brain and spinal cord exhibit distinct sensitivities to cellular mediators of tissue damage, and IL-17 and IFN-γ differentially regulate recruitment of these mediators to each microenvironment. These data suggest that the specific region targeted by inflammatory lesions in individual patients may predict their response to therapies that neutralize cytokine activity.

Contents

List of Abbreviations

APC	Antigen-presenting cell
CNS	Central Nervous System
EAE	Experimental autoimmune encephalomyelitis
GWAS	Genome wide association studies
IFN-γ	Interferon gamma
IL-17	Interleukin 17
IL-1β	Interleukin-1 beta
IL-17RA$^{-/-}$	Interleukin-17 receptor A knock-out
IFN-γR-/-	Interferon gamma receptor alpha knock-out
MAG	Myelin-associated glycoprotein
MHC	Major histocompatibility complex
MOG	Myelin oligodendrocyte glycoprotein
MS	Multiple Sclerosis
NMO	Neuromyelitis optica
NOD	Non-obese diabetic
PARP-1	Poly(ADP-ribose) polymerase 1
PP-MS	Primary progressive multiple sclerosis
RR-MS	Relapsing-remitting multiple sclerosis
SC	Spinal cord
SP-EAE	Secondary progressive experimental autoimmune encephalomyelitis
SP-MS	Secondary-progressive multiple sclerosis
Th1	Interferon gamma producing T helper cell
Th17	IL-17 producing T helper cell
TMEV	Theiler's murine encephalomyelitis virus
WT	Wild-type

List of Figures and Tables

Chapter 1- Overview of MS

Multiple sclerosis (MS) is a demyelinating disease of the central nervous system (CNS), estimated to affect up to two million people worldwide. Hallmarks of MS include focal inflammatory infiltrates, demyelinating plaques, and axonal damage. While the etiology of MS is not known, it is widely considered to be an autoimmune disease. Recent genome-wide association studies (GWAS) provided strong support for this notion by identifying >100 susceptibility loci associated with MS of which the vast majority represent genes with immune cell function [1]. A long-standing hypothesis for the etiology of MS is that environmental factors trigger MS in genetically susceptible individuals by promoting the activation of myelin-specific T cells that normally circulate in the periphery of healthy individuals in a tolerant state. Once activated, these T cells can enter the CNS and initiate an autoimmune response. A major role for $CD4^+$ T cells in this process is strongly supported by the observation that the strongest association of genetic susceptibility to MS is with MHC class II alleles that present antigen to $CD4^+$ T cells. However, a role for MHC class I alleles that present antigen to $CD8^+$ T cells was also confirmed by these GWAS studies, suggesting a complex pathogenesis [1].

Developing therapies to treat or prevent MS requires an in-depth understanding of the pathogenesis of the disease. Mechanistic studies in MS are difficult because CNS tissue is difficult to access and immune responses within this tissue cannot be easily monitored. Therefore, animal models are essential in defining the mechanisms underlying MS. These models are important not only to discover new therapeutic targets, but also to test new therapies prior to translation to patients. One of the major challenges in developing animal models of MS is that patients with MS vary widely both in disease presentation and in response to therapeutics.

Examples of such heterogeneity in disease include the type of clinical signs (which reflect location of inflammatory plaques [2]), disease course (occurrence of remissions and relapses) [3], and pathological features [4]. This extensive heterogeneity raises the question: does MS have a single etiology, made heterogeneous by genetics and environment, or is MS a syndrome resulting from various pathogenic pathways? The question remains to be answered, yet has important ramifications on treatment decisions. Developing animal models that recapitulate different aspects of the disease seen in patients with MS may shed important light on this issue.

The clinical disease course varies among patients with MS

Patients with MS can be subcategorized based on distinct clinical patterns. About 85% of patients with MS develop relapsing-remitting MS (RR-MS), during which patients experience episodes of neurological disability but return to baseline following relapse. Approximately 50% of these RR-MS patients later develop a clinically distinct form of disease referred to as secondary progressive MS (SP-MS) within 10 years of onset of RR-MS [5]. In SP-MS, periods of remission still occur but the steady-state level of clinical disability during remission worsens over time and, importantly, brain atrophy steadily increases [6]. The reasons for this shift to steadily increasing clinical disability and lack of return to baseline are not known. Interestingly, even though patients may convert from RR-MS to SP-MS at different times following the initial diagnosis, once a patient converts to SP-MS, the overall increase in disability and in brain atrophy proceed at the same rate [3]. This suggests that there may be a mechanistic shift in the pathogenesis that occurs when a patient converts to SP-MS. Mechanisms underlying secondary progressive disease have recently been proposed [3]. While inflammatory lesions that are detected by MRI during RR-MS are less apparent by imaging techniques during SP-MS, some

inflammatory immune cells may still be engaged in tissue destruction but are not detected by imaging because the blood brain barrier is no longer permeable.

There is also a form of MS called primary progressive (PP-MS), which comprises approximately 10-20% of all MS cases. Patients with PP-MS lack the acute exacerbations seen in patients with RR-MS; instead, they develop steadily worsening clinical disability from the time of their initial diagnosis [7]. Patients with PP-MS respond poorly to most commonly used immune-modulating MS therapeutics [8], suggesting that a different pathogenic pathway may be at play in these patients compared to those with RR-MS. Key differences between PP-MS and SP-MS also exist, including age at onset, initial symptoms, and ratio of males to females [9], however they are often grouped together and collectively referred to as progressive MS based on their similarities. In patients with both SP-MS and PP-MS, focal plaques of demyelination are common, but classical actively demyelinating plaques like those commonly seen in RR-MS are rare. Both also demonstrate increased atrophy, axonal loss, and cortical demyelination with extensive diffuse injury in the normal-appearing white matter [8]. In addition, PP-MS and SP-MS have fewer gadolinium enhancing MRI lesions compared to RR-MS [10], however, profound differences in MRI patterns were seen between patients with PP-MS and SP-MS [11]. Overall, MRI and pathological data show both similarities and differences between PP-MS and SP-MS, but ultimately, it remains to be seen whether future therapeutics will provide similar benefits to patients with SP-MS and PP-MS. To date, no therapies have shown benefit in patients with PP-MS, and only IFNβ-1b and mitoxantrone have been approved for patients with SP-MS [10].

Patients with MS exhibit diverse pathological features

The CNS pathology in MS is characterized by inflammatory lesions, plaques of demyelination, remyelination, neurodegeneration, and glial scar formation [3]. Most actively demyelinating MS lesions are dominated by macrophages containing myelin degradation products and T cells, while inactive or chronic active plaques contain microglia and macrophages without myelin degradation products [12]. Beyond these "hallmark" features, substantial heterogeneity is observed in the CNS pathology. Criteria have been developed that allow the lesions seen in patients with MS to be divided into four categories (Patterns I-IV). The criteria are based on the distribution of myelin loss, plaque geography and extension, pattern of oligodendrocyte injury, and immunopathological evidence of immunoglobulin and activated complement deposits [4]. Patterns I and II lesions share a perivenous distribution of plaques dominated by T cells and macrophages with preservation of oligodendrocytes. The main difference between pattern I and pattern II lesions is the presence of immunoglobulin and complement deposits in pattern II lesions. In contrast, patterns III and IV are associated with oligodendrocyte cell death, and did not preferentially occur around vessels. In pattern III, oligodendrocytes undergo apoptosis while in pattern IV, non-apoptotic cell death is observed. Pattern III is unique in that there appears to be a preferential loss of myelin-associated glycoprotein (MAG) from damaged myelin. These pattern III lesions are suggested to resemble hypoxic/ischemic white matter damage [13]. In general, pattern I and II lesions appear to be consistent with a T cell or T cell plus antibody-mediated autoimmune pathology, while pattern III and IV lesions are more consistent with primary oligodendrocyte dystrophy, such as from ischemic, viral, or toxin-induced demyelination. Pattern II lesions are most prevalent, found in 58% of patients with MS, followed by pattern I (26%), pattern III (15%), and pattern IV lesions (1%) [14]. Interestingly, pattern I

and II lesions appeared in patients with all clinical subtypes (RR-MS, SP-MS, and PP-MS), while pattern IV lesions occurred exclusively in patients with PP-MS. Patients with pattern III lesions were found mainly in patients with disease duration less than two months [4].

One of the most important findings to come from these studies is that multiple active plaques analyzed from an individual belong to the same pattern, indicating a lack of intra-individual heterogeneity. This suggests that the pathological patterns may reflect distinct pathogenic pathways occurring in different individuals rather than the evolution of lesions over time within an individual [4]. This notion emphasizes the importance of developing biomarkers to stratify patients with MS into distinct groups so that treatment protocols are appropriately matched to the pathogenic mechanisms relevant to their disease.

Lesion localization differs between patients with MS

The locations of lesions within the CNS are the major determinant of clinical signs, and these are also variable among patients. Lesions in the majority of patients are found throughout the brain, particularly in the periventricular white matter, cerebellum, brainstem, and optic nerves. Although historically considered a disease of the white matter tracts, cortical and deep gray matter lesions are also common in patients with RR-MS, and become more prominent and extensive in patients with both PP-MS and SP-MS, correlating with irreversible disability [14]. These lesions are undetectable in live patients by conventional imaging, but likely contribute to the cognitive impairment and seizures experienced by some.

Although most patients with MS have lesions in the brain with or without accompanying spinal cord involvement, 2-10% of patients exhibit inflammation in the spinal cord and/or optic nerves without extensive involvement of the brain [15, 16]. Spinal cord-dominated disease is

particularly common in, but not restricted to, patients with MS of Asian descent (termed Asian-type opticospinal MS), and there is currently some debate as to whether Asian-type opticospinal MS is distinct from neuromyelitis optica (NMO) (otherwise known as Devic's disease) [17]. An antibody specific for aquaporin-4 is found in a high proportion of patients with NMO; recently, this antibody was also found in Asian patients with opticospinal MS, but not in patients with MS from North America that exhibit the more common pattern of brain lesions [18]. Regardless of whether NMO and Asian-type opticospinal MS are distinct entities, they share a predilection for inflammation localized to the spinal cord, in contrast to the majority of patients with MS, in which inflammation targets the brain in addition to the spinal cord. These distinct localization patterns suggest that mechanisms promoting inflammation in the brain may be distinct from lesions promoting inflammation in the spinal cord.

Chapter 2- Overview of EAE

The oldest and most widely used animal model for MS is experimental autoimmune encephalomyelitis (EAE). EAE has been studied in a variety of animal species, including mouse, rat, rabbit, guinea pigs, and non-human primates. EAE is induced either by immunization with myelin antigens (active induction) or by adoptive transfer of activated T cells isolated from animals immunized with myelin antigens (passive induction) [19, 20]. The manifestation of EAE can vary greatly depending on the strain or genotype of rodent and sometimes the mode of induction (active versus passive). Although differences between EAE models can occasionally confound results and make interpretations difficult, they also can shed light on the complexity and heterogeneity of CNS autoimmune disease. No single model replicates the full spectrum of inflammatory mechanisms and neurodegeneration seen in MS, just as individual patients manifest only a subset of the diverse features of the disease. The following EAE models, summarized in Table 1, replicate certain features seen in patients with MS, and therefore may be valuable tools in understanding this heterogeneous disease.

Models of different clinical manifestations of MS

EAE models exist with clinical course similar to RR-MS

EAE induced in SJL mice models the relapsing-remitting pattern of clinical signs seen in patients with RR-MS. Mechanistic studies in these SJL mice have provided one explanation for relapsing-remitting clinical course. Analysis of the specificity of T cells infiltrating the CNS over time demonstrated a phenomenon known as epitope spreading, in which some naïve T cells that are non-specifically recruited to the CNS by inflammatory signals are activated by encounter with myelin epitopes generated during tissue damage. These epitopes are distinct from the original epitope targeted by T cells that initially induced disease [21-23]. Activation of these T

cells specific for different myelin epitopes are hypothesized to trigger new waves of autoimmune T cell responses that promulgate the disease and induce relapse following remission in mice. Thus, epitope spreading may explain how recurring autoimmune responses in RR-MS are propagated over time [24]. Importantly, it has been shown that initially tolerizing T cell responses to epitopes expected to occur later in the immune response can prevent relapses [25]. Other animal models have also suggested that epitope spreading contributes to CNS autoimmunity. Infection of mice with the demyelinating virus Theiler's murine encephalomyelitis virus (TMEV) leads to infiltration of virus-specific T cells that facilitate tissue damage as they eliminate virally infected cells. As a result of this tissue damage, myelin epitopes are presented by APCs during TMEV infection [26], and T cells specific for myelin epitopes expand in the CNS later in infection and promulgate an autoimmune response [27]. The notion of epitope spreading provides a satisfying explanation for the chronicity of the autoimmune response in the CNS. However, this theory is somewhat controversial. Others have reported that the dominant T cell response remains directed toward the priming epitope throughout relapses [28], and that relapses can be prevented by depleting the transferred T cells that initiated disease but not host cells that would contribute to epitope spreading [29]. The basis for the occurrence of relapses in patients with MS has yet to be fully understood.

Other relapsing/remitting EAE models have also been described. C57BL/6 mice can develop a relapsing-remitting course when disease is induced with low doses of MOG 35-55 [30], or when the saponin extract Quil A is used as an adjuvant [31] in place of complete Freund’s adjuvant. The mechanisms responsible for relapses in these models have not been identified.

EAE models exist which exemplify some aspects of SP-MS

A change in pathogenic mechanisms is hypothesized to occur when patients with MS transition from RR- to SP-MS. As discussed above, inflammation in the CNS (at least as detected by imaging techniques) decreases while brain atrophy and axonal loss steadily increase. Accordingly, patients with SP-MS do not respond to immunosuppressive reagents [8]. Thus, new therapies that focus on neuroprotective strategies may be needed.

A few EAE models exist that exemplify characteristics of SP-MS, which may be useful in identifying new therapeutic strategies for patients in this stage of disease. Biozzi ABH mice initially develop relapsing-remitting disease which then transitions to a steadily progressive disease course [32]. In addition, NOD mice induced for EAE demonstrate a partial recovery after the initial acute phase that is followed by a chronic progressive disease course [33]. Significant axonal and neuronal loss are found in both NOD and Biozzi mice with chronic progressive EAE, similar to patients with SP-MS. As in patients with SP-MS, immunosuppressive strategies fail to ameliorate secondary progressive EAE (SP-EAE) in these models. For example, immunosuppression by FTY720 ameliorates disease in the RR but not in the SP phase of Biozzi mice [34]. Additionally, an immunosuppressive strategy of $CD4^+$ T cell depletion combined with an agent designed to promote tolerance to CNS antigens was able to halt relapses, but not subsequent progression of disability in the Biozzi relapsing-progressive model of EAE [35]. Importantly, neuroprotective therapeutic approaches have offered some promise in SP-EAE models. Axon loss and clinical progression were reduced in NOD mice with progressive EAE following treatment with the neuroprotective agent ABS-75, despite demonstrating no effect in traditional relapsing and monophasic EAE models [33]. In addition, the Toll-like receptor 2 and poly(ADP-ribose) polymerase 1 (PARP-1) pathways have been identified as potential new

therapeutic targets using this same progressive EAE model in NOD mice [36]. 15α-hydroxycholestine (an activator of the PARP-1 pathway) is increased in patients with SP-MS and NOD mice with SP-EAE, and the PARP-1 inhibitor 5-aminoiso-quinolinone (AIQ) inhibited clinical signs, axonal loss and demyelination in NOD mice with SP-EAE. Whether inhibition of this pathway is efficacious in patients with SP-MS remains to be seen.

In addition to the Biozzi and NOD models of progressive EAE, SP-EAE models have been induced in the SJL/J and A.SW strains of mice. SJL/J mice typically develop a relapsing-remitting disease course upon immunization with MOG_{92-106}, but following UV irradiation, about 20% of mice develop SP-EAE, which is characterized by a large number of apoptotic cells in lymphoid organs [37]. Interestingly, MOG_{92-106}-immunized A.SW mice injected with *Bordetella pertussis* toxin also developed SP-EAE characterized by atrophic spleens [38]. Together, these models led to the hypothesis that apoptotic lymphocytes may themselves result in progressive disease, which was supported by the observation that SP-EAE was induced by injection of apoptotic thymocytes themselves [37]. These SP-EAE models were characterized by large demyelinating lesions with fewer infiltrating T cells and increased macrophage and polymorphonuclear cells compared to RR-EAE models. SP-EAE also had higher titers of anti-MOG antibodies in the serum and decreased IFN-γ production by splenocytes, suggesting that lymphoid apoptosis may alter the balance of T cell cytokines and increase anti-MOG antibody responses leading to disease progression. Support for such pathways in patients with SP-MS are evident by detection of ectopic B cell follicles with germinal centers in the meninges of these patients [39]. Furthermore, retrospective analysis of the anti-CD20 antibody Rituximab in patients with SP-MS supports the therapeutic efficacy of B cell depletion [40], and clinical trials

of this therapy in SP-MS are currently underway (http://www.ninds.nih.gov/disorders/clinical_trials/NCT01212094.htm).

Some animal models reflect differences in lesion pathology seen in patients with MS

The pathological features of classic EAE models are most reminiscent of patterns I and II lesions in MS [4], and support the idea that pattern I and II lesions may result primarily from the activity of T cells and macrophages. As pattern II MS lesions are also distinguished by immunoglobulin and activated complement deposits, B cells and complement likely play a pathogenic role in patients with this pattern of lesions. Similarly, B cells appear to contribute to the pathogenesis in some, but not all, EAE models. Unlike pattern I and II lesions, pattern III and IV lesions resemble a primary oligodendrocyte dystrophy, demonstrating a high degree of oligodendrocyte cell death with resulting demyelination. Similarities to pattern III and IV pathology were reported in a $CD8^+$ T cell-mediated EAE model [41]; however, this type of primary oligodendrocyte damage is seen more in cuprizone-induced demyelination models [42, 43] or virus-induced demyelination in mice [44], than in commonly used EAE models. This supports the theory that varying mechanisms of disease exist for the different pathological subsets and warrants personalizing treatment protocols based on pathology criteria.

Atypical and classic EAE models represent different inflammatory patterns seen in patients with MS

As discussed above, most patients with MS develop lesions in the brain with or without accompanying spinal cord lesions. Only a subset of patients exhibit a form of MS in which lesions are found primarily in the spinal cord and optic nerves with relative sparing of the brain.

Unexpectedly, most mouse EAE models exhibit an inflammatory pattern similar to this subset of patients, in which parenchymal lesions are found predominantly in the spinal cord and optic nerve with relatively little inflammation in the brain parenchyma. This pattern of spinal cord tissue injury accounts for the clinical signs of ascending flaccid paralysis associated with classic EAE models. In the 1980s and 1990s, however, reports began to emerge of EAE models in which mice showed signs of what was referred to as "vestibular-type" or "non-classical" EAE [45, 46]. These "non-classical" EAE mice were characterized by atypical symptoms of head tilt, spinning, or axial rotation. The significance of these atypical symptoms was unclear until 2000, when Muller et al. reported that atypical signs correlate with inflammation in the brain (particularly the brainstem and cerebellum), while classical symptoms correlated with spinal cord inflammation. Atypical EAE (and parenchymal brain inflammation) occurred only in EAE models that utilized specific mouse strains and antigen combinations. These studies suggested that conditions leading to inflammation in the spinal cord were not sufficient to promote inflammation in the brain, and were the first indication in animal models of CNS autoimmunity that the brain and spinal cord are distinct microenvironments with different requirements for inflammation. Studies of both atypical and classic EAE models have identified some mechanisms that lead to inflammation in the brain versus the spinal cord, and may help illuminate mechanisms underlying the varying lesion localization patterns among patients with MS, as discussed further below.

IL-17 and IFN-γ influence neuroinflammatory patterns during EAE

$CD4^+$ T cells play an essential role in EAE initiation and are thought to be important players in the pathogenesis of MS. $CD4^+$ T cells can be subcategorized based on the types of cytokines they

produce; two well-studied $CD4^+$ T cell subsets in EAE are T_H1 (IFN-γ producing) and T_H17 (IL-17 producing) cells. The T_H17-associated cytokine IL-17 and T_H1-associated cytokine IFN-γ have both been extensively studied in various EAE models. Initially, IFN-γ was hypothesized to be the main pathogenic cytokine in EAE based on the finding that T_H1 cells were capable of inducing disease [47, 48] and IFN-γ was secreted by CNS-infiltrating T cells in EAE [49, 50]. However, this was disproven upon discovery that T_H1-associated factors, including IL-12 [51, 52] and IFN-γ [53] were not required for disease induction. Upon discovery that the T_H17-promoting cytokine IL-23 was required for EAE development, T_H17 cells were then considered to be the main cells responsible for EAE pathogenesis. Subsequent studies found that IL-17 promotes disease in some [54-57], but not all [58-60] models of EAE. Although neither IL-17 nor IFN-γ appear to be required for EAE development, they play important roles in differentially regulating inflammatory responses in the brain and spinal cord. The ability of IFN-γ signaling to determine lesion localization independent of antigen specificity was clearly illustrated in a TCR transgenic model in which a monoclonal myelin-specific TCR was expressed on a wild-type or IFN-$\gamma^{-/-}$background [61]. $Rag^{-/-}$ MBP TCR transgenic mice developed spontaneous EAE typified by spinal cord inflammation and classic symptoms of ascending flaccid paralysis. However, when these mice were backcrossed to an IFN-$\gamma^{-/-}$background, they developed a "non-classical EAE" characterized by brain inflammation and atypical symptoms. This suggested that IFN-γ suppressed inflammation in the brain but not in the spinal cord. In fact, spinal cord inflammation appeared less severe in the MBP TCR transgenic mice on the IFN-$\gamma^{-/-}$ background, as lower numbers of $CD4^+$ T cells and total cellularity were observed in spinal cords of mice lacking IFN-γ compared to wild-type mice [61].

Subsequent studies confirmed the suppressive effect of IFN-γ on brain inflammation. Two groups have demonstrated that polyclonal T cells isolated from IFN-$\gamma^{-/-}$ mice induce an atypical disease when transferred into wild-type hosts [58, 62]. The study by Lees et al. showed that MOG-specific, but not OVA-specific, wild-type T_H1-skewed cells were able to suppress the brain inflammation induced by the IFN-$\gamma^{-/-}$T cells [62]. This group also showed that the suppressive ability of IFN-γ in the brain is dependent on host cells receiving a signal from IFN-γ, as wild-type T cells transferred into IFN-γR$^{-/-}$ hosts also induced brain inflammation and atypical EAE. Their results were also consistent with the finding of Wensky et al. [61] that IFN-γ signaling has a non-redundant, pro-inflammatory effect in the spinal cord as IFN-$\gamma^{-/-}$ T cells induced less disease in the spinal cords of WT mice compared to wild-type T cells [63]. The mechanisms by which IFN-γ exerts differential effects throughout the CNS (inhibiting inflammation in the brain while promoting inflammation in the spinal cord) were not identified by these studies.

Other models of atypical EAE have been described that do not depend on IFN-γ deficiency. For example, certain H-2^k mouse strains generate PLP-specific T cells that preferentially induce lesions in the brainstem and cerebellum [64]. This was hypothesized to reflect either the ability of these particular peptide/MHC ligands to elicit T cells whose cytokine production promoted brain inflammation or differential processing of myelin antigen in different CNS compartments.

Subsequent studies in our lab using an alternate model of atypical disease revealed that the priming epitope influences effector cytokines produced by T cells, and that these cytokines contribute to lesion localization [59]. T_H17 cells in particular were implicated as important promoters of brain inflammation. These studies in C3HeB/Fej mice showed that EAE was

strongly affected by the abundance of T_H1 and T_H17 cells within the T cell population infiltrating the CNS. We found that inflammation in the spinal cord was induced by transferring T cells with a wide range of T_H17:T_H1 ratios; however, inflammation in the brain was induced only when the T_H17:T_H1 ratio was ≥ 1 [59]. Blockade of IL-17 signaling via neutralization of IL-17 activity [59] ameliorated brain but not spinal cord inflammation in this atypical EAE model. Additionally, atypical EAE that developed in C57Bl/6 mice following adoptive transfer of IFN-$\gamma^{-/-}$ T cells converted to classic EAE in IL-17RA$^{-/-}$ recipients [58]. These findings demonstrate that T_H17 cells and IL-17 signaling strongly promotes inflammation in the brain, while IFN-γ signaling inhibits inflammation in this region. The mechanism by which these cytokines influence brain inflammation was not identified in these studies. In the following chapters, I describe the mechanistic basis for the differential activities of IL-17 and IFN-γ in the brain and spinal cord by demonstrating that IL-17 promotes, while IFN-γ inhibits ELR$^+$ chemokine-mediated neutrophil recruitment to the brain, which is required for the development of parenchymal brain lesions. I also show that the brain and spinal cord function as distinct microenvironments, with differing responses to IL-17 and IFN-γ signaling and discuss therapeutic implication of these findings for treatment of patients with MS.

Table 1. Different animal models replicate various aspects of MS

Clinical Course

	Model System	Strain:Antigen	References
Relapsing-Remitting	Wild-type mice	SJL/J: $PLP_{131-151}$	[65]
	Transgenic TCR^{MOG}	SJL/J: MOG_{92-106} (spontaneous)	[66]
	Wild-type mice, adjuvant specific	C57BL/6:MOG_{35-55} (adjuvant Quil A)	[31]
	Wild-type mice, antigen/adjuvant dose specific	C57BL/6: MOG_{35-55} (low dose)	[30]
Secondary Progressive	Wild-type mice, +UV irradiation or apoptotic thymocytes	SJL/J:MOG_{92-106}	[38]
	Wild-type mice, + *Bordetella pertussis*	A.SW:MOG_{92-106}	[37]
	Wild-type mice	Biozzi ABH: spinal cord homogenate	[32]
	Wild-type mice	NOD: MOG_{35-55}	[33]

Pathological Pattern

	Model System	Strain:Antigen	References
Pattern I /II	Most CD4-mediated EAE Models		[2]
Pattern III/ IV	Wild-type mice (CD8 T cell clones)	C3H/Fej: MBP_{79-87}	[41]
	Cuprizone-induced demyelination	C57BL/6, Swiss Webster	[42, 43]
	TMEV-induced demyelination	SJL/J	[44]

Lesion Localization

	Model System	Strain:Antigen	References
Spinal Cord	Most EAE models although IFN-γ deficiency lessens spinal cord lesions in some models		
Opticospinal	Transgenic TCR^{MOG} x IgH^{MOG}	C57BL/6: MOG (spontaneous)	[67, 68]
Brain (+/- Spinal Cord)	IFNγ or IFNγR deficiency	Multiple	[58, 61, 62, 69]
	Wild-type mice	CBA/J: $PLP_{190-209}$	[64]
	Wild-type mice	C3H/Hej: $PLP_{190-209}$	[46]
	Wild-type mice	C3HeB/Fej: MOG_{97-114}	[70]
	Transgenic TCR^{MOG}	SJL/J: MOG_{92-106} (spontaneous)	[66]
	Wild-type mice (CD8 T cell clones)	C3H/Fej: MBP_{79-87}	[41]

Chapter 3- IL-17 and IFN-γ signaling differentially influence inflammation in the brain and spinal cord

Clinical manifestation of EAE is determined by IL-17 and IFN-γ signaling

As described above, our laboratory previously showed that WT C3HeB/Fej mice exhibit atypical EAE because MOG_{97-114} T cells primed by immunization with MOG in this strain exhibit a high T_H17:T_H1 ratio that was required to induce inflammation in the brain. The critical role of the T_H17:T_H1 ratio was demonstrated by showing that T cells specific for other MOG epitopes that normally induced classic EAE could induce atypical EAE when their T_H17:T_H1 ratio was increased by skewing the T cells *in vitro* toward a T_H17 phenotype. Administrating soluble IL-17RA-Ig to these mice ameliorated atypical EAE signs, suggesting that IL-17 signaling was critical for promoting brain inflammation [59].

The T_H17-associated cytokines IL-17A and IL-17F are members of the IL-17 family that share 56% sequence homology and can act as homodimers or heterodimers to signal through a heterodimeric complex made up of IL-17 receptor family members IL-17RA and IL-17RC [71]. IL-17A and IL-17F homo- and heterodimers trigger Act1-dependent NFkB activation required for the induction of downstream inflammatory genes. IL-17RA is ubiquitously expressed and is required for functional signaling of both IL-17A and IL-17F, as well as other members of the IL-17 family including IL-17C and IL-17E [72].

IFN-γ also signals via two functional receptors, IFN-γRα (also known as IFN-γR1) and IFN-γRβ (also known as IFN-γR2). IFN-γ binds and dimerizes two IFN-γRα molecules, which

prompts the association of two IFN-γRβ molecules that in turn leads to the phosphorylation and activation of STAT-1. These STAT-1 dependent pathways are the most well-known and well-studied of IFN-γ's activity, although STAT-1 independent pathways also exist [73], as will be discussed later. Both IFN-γRα and IFN-γRβ are required for functional IFN-γ signal transduction to occur.

Here we employed recipient mice genetically deficient in IL-17RA, IFN-γRα (IFN-γR$^{-/-}$), or both IL-17RA and IFN-γR (IL-17RA$^{-/-}$x IFN-γR$^{-/-}$) to define the precise roles of IL-17 and IFN-γ signaling in determining lesion localization and clinical manifestation of EAE. These models allow us to ascertain the precise role of cytokine signaling in the host following disease induction. EAE was induced by transfer of WT CD4+ T cells skewed toward a T_H17 phenotype *in vitro* (T_H17:T_H1 ratio of ~2:1, data not shown) in order to predispose the WT recipients toward atypical EAE and to bypass any potential effects of IL-17 or IFN-γ signaling on development or priming of myelin-specific T cells. The overall EAE incidence (defined as the percentage of mice with atypical and/or classic EAE signs) was modestly reduced in both IFN-γR$^{-/-}$mice and IL-17RA$^{-/-}$ mice (**Fig. 1a**). However, EAE incidence was strongly reduced in IL-17RA$^{-/-}$x IFN-γR$^{-/-}$ double knock-out mice (**Fig**. **1a**), indicating that preventing signaling via both cytokine receptors has a much greater impact on overall incidence than preventing signaling via either cytokine receptor alone. Importantly, deficiency in either cytokine receptor had a strong effect on clinical manifestation of disease. In IL-17RA$^{-/-}$ mice that developed EAE, both the severity and incidence of atypical signs was sharply reduced compared to WT mice (**Fig. 1b, c**), supporting our previous finding that IL-17 signaling promotes atypical EAE [59]. However, the severity and incidence of classic EAE signs among these same mice was unchanged (**Fig. 1b, d**). In contrast, IFN-γR$^{-/-}$ recipients of IL-23-skewed T cells demonstrated similar severity but increased

incidence of atypical EAE signs compared to WT mice (**Fig. 1e, f**), consistent with other reports that IFN-γ signaling inhibits the incidence of brain inflammation [58, 61, 62]. Interestingly, both the severity and incidence of classic EAE in these same mice was significantly reduced compared to WT recipients (**Fig. 1e, g**), supporting the notion that IFN-γ promotes inflammation in the spinal cord [58, 61, 62], despite its inhibitory effect in the brain. Collectively, these data indicate that both IL-17 and IFN-γ signaling promote overall EAE development, but do so by differentially influencing the development of atypical versus classic EAE signs.

Of note, IFN-γ signaling also influenced the timing of disease onset. IFN-γR$^{-/-}$ recipients developed clinical signs on average 2.4 days later than WT recipients (**Fig. 1e**), although the variation in disease onset in IFN-γR$^{-/-}$ mice was quite large. While disease onset in WT mice ranged between day 5 and day 8, IFN-γR$^{-/-}$ mice developed EAE signs as early as day 5 and as late as day 22. The reason underlying the difference in the time of disease onset between WT and IFN-γR$^{-/-}$ mice is unclear. It is also not clear why there is a broader range in the day of disease onset in IFN-γR$^{-/-}$ mice.

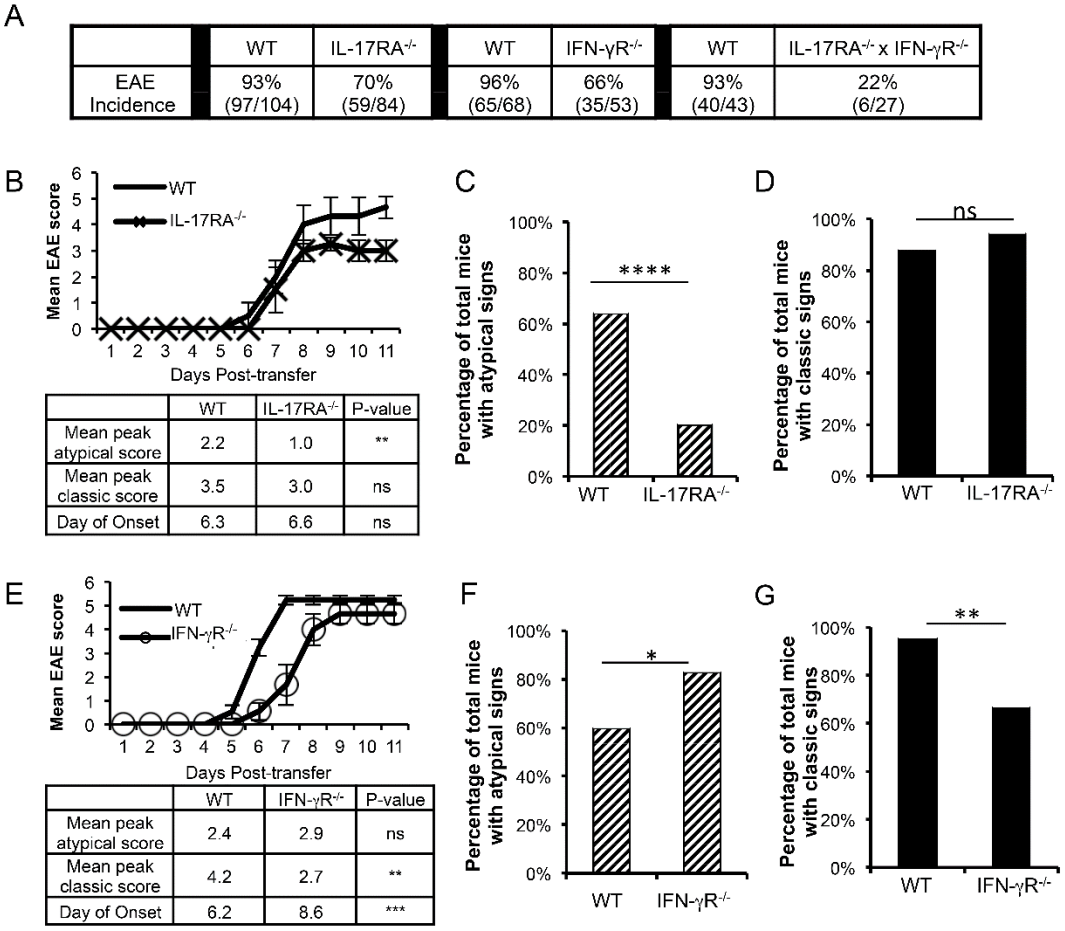

Figure 1. IL-17 and IFN-γ signaling influence clinical manifestation of EAE. (A) Overall incidence of disease is shown for EAE induced by adoptive transfer of IL-23-skewed WT T cells into wild-type (WT), IL-17RA$^{-/-}$, IFN-γR$^{-/-}$ and IL-17RA$^{-/-}$xIFN-γR$^{-/-}$ recipients. The number of WT mice used as controls for transfers into recipients of each genetic background is indicated. **(B)** Representative disease course for 5 IL-17RA$^{-/-}$ and 6 WT recipients is shown (top) and clinical characteristics are summarized for all 59 IL-17RA$^{-/-}$ and 97 WT control recipients with EAE (bottom). Clinical data are compiled from 8 independent experiments. (**C)** The percentage of mice with EAE that exhibited atypical clinical signs with or without accompanying classic

clinical signs is shown for the 59 IL-17RA$^{-/-}$ and 97 WT control recipients. **(D)** The percentage of the same mice shown in (C) that exhibited classic EAE signs with or without accompanying atypical EAE signs is shown. **(E)** Representative disease course for 9 IFN-γR$^{-/-}$ and 13 WT recipients is shown and clinical characteristics are summarized for all 35 IFN-γR$^{-/-}$ and 65 WT control recipients with EAE. Data are compiled from 4 independent experiments. **(F)** The percentage of mice that exhibited atypical clinical signs with or without accompanying classic signs is shown for the 35 IFN-γR$^{-/-}$ and 65 WT control recipients with EAE. **(G)** The percentage of the same mice shown in (F) that exhibited classic EAE signs with or without accompanying atypical EAE signs is shown. *NS, not significant; * P< .05; ** P< .01; **** P< .0001.*

IFN-γ inhibits and IL-17 induces neutrophil recruitment to the brain

To dissect the mechanisms by which IL-17 and IFN-γ signaling exert opposite effects on induction of brain inflammation, we analyzed the inflammatory infiltrate in the brains of WT, IL-17RA$^{-/-}$ and IFN-γR$^{-/-}$ recipients of IL-23-skewed MOG$_{97-114}$-specific T cells at peak disease (day 7-8 post-transfer, gating strategy shown in **Supplementary Fig. 1**). Flow cytometric analyses showed that the number of inflammatory monocytes (CD45^{+}CD11b^{+}Ly6C^{hi}) was similar in the brains of WT, IL-17RA$^{-/-}$ and IFN-γR$^{-/-}$recipients (**Fig. 2a, b**). In contrast, the number of neutrophils (identified as CD45^{+}CD11b^{+}Ly6G^{+} cells) in the brain was significantly decreased in IL-17RA$^{-/-}$ recipients (**Fig. 2a**) and significantly increased in IFN-γR$^{-/-}$mice (**Fig. 2b**), correlating with the incidence of atypical signs in these mice. Although the differences were less dramatic, the absolute number of CD4^{+} T cells (identified as CD45^{+}TCR^{+}CD4^{+} cells) in the brain tended to be lower in IL-17RA$^{-/-}$ mice but was significantly increased in IFN-γR$^{-/-}$recipients compared to WT recipients. However, initial CD4^{+} T cell infiltration was not impaired in the absence of IL-17 signaling as the CD4^{+} T cell number was actually higher in the brains of IL-17RA$^{-/-}$ compared to WT mice during preclinical disease (day 4 post-transfer, **Fig. 2c**). Together, these data suggest that neutrophil infiltration of the brain correlates with T cell recruitment in the brain and manifestation of atypical clinical signs during EAE.

ELR+ chemokines are chemoattractants for neutrophils that facilitate their trafficking to inflamed tissues, and are induced in response to inflammatory cytokines such as IL-17 and IL-1β [74]. We hypothesized that differences in ELR+ chemokine expression caused by deficiency in either IL-17 or IFN-γ signaling during EAE may account for the differences in neutrophil accumulation in the brains of IL-17RA$^{-/-}$ versus IFN-γR$^{-/-}$ mice. We first analyzed the expression of ELR+ chemokines by quantitative PCR in the brain in WT mice with EAE. We found that

CXCL1, CXCL2, and CXCL5 were induced in brains of EAE mice compared to healthy control brains. Notably, CXCL2 was induced to the greatest extent (5-fold higher than CXCL1 and approximately 100-fold higher than CXCL5, **Fig. 2d**). Expression of these chemokines was significantly decreased in the brains of IL-17RA$^{-/-}$ mice (**Fig. 2e**), consistent with the ability of IL-17 to promote ELR+ chemokine expression. In contrast, CXCL2 expression trended higher in the brains of IFN-γR$^{-/-}$mice (**Fig. 2e**), which may account for the greater accumulation of neutrophils in the brain in IFN-γR$^{-/-}$mice compared to WT mice (**Fig. 2b**). Together these data suggest that the differential recruitment of neutrophils to the brain in IL-17RA$^{-/-}$ versus IFN-γR$^{-/-}$ mice reflects the ability of IL-17 signaling to strongly promote expression of CXCL1, CXCL2 and CXCL5 as well as the potential for IFN-γ signaling to inhibit CXCL2 expression.

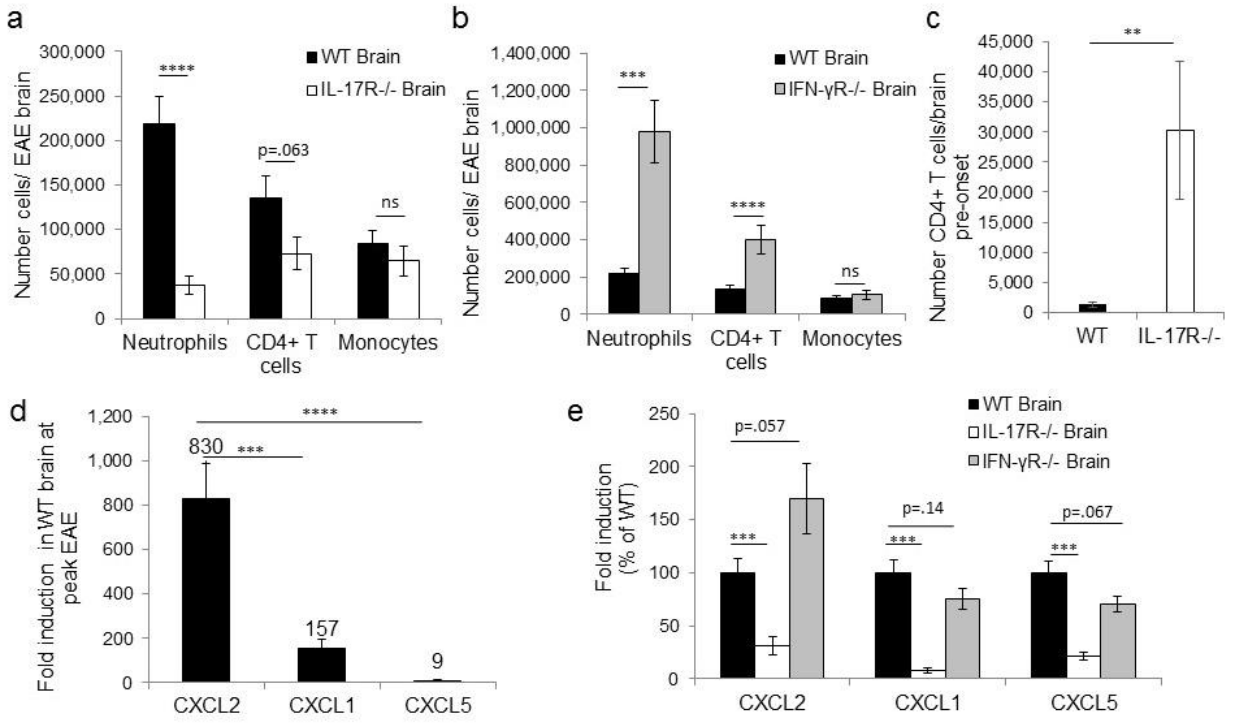

Figure 2. IL-17 signaling promotes, while IFN-γ signaling inhibits, neutrophil accumulation and CXCL2 induction in the brain. (a) The absolute number of neutrophils (WT, n=23; IL-17RA$^{-/-}$, n=10), CD4^{+} T cells (WT, n=23; IL-17RA$^{-/-}$, n=10), and inflammatory monocytes (WT, n=15; IL-17RA$^{-/-}$, n=6) are shown for cells isolated from the brains of WT and IL-17RA$^{-/-}$ mice with EAE ≥ grade 3. Data are compiled from 2-7 independent experiments. **(b)** The absolute number of neutrophils (WT, n=23; IFN-γR$^{-/-}$, n=13), CD4^{+} T cells (WT, n=23; IFN-γR$^{-/-}$, n=11), and inflammatory monocytes (WT, n=15; IFN-γR$^{-/-}$, n=7) are shown for cells isolated from the brains of WT and IFN-γR$^{-/-}$ mice with EAE ≥ grade 3. Data are compiled from 3-7 independent experiments. **(c)** The absolute number of CD4^{+} T cells are shown for cells isolated from the brains of WT (n=4) and IL-17RA$^{-/-}$ (n=4) mice prior to EAE onset (day 4). Data are representative of 2 independent experiments. **(d)** Fold induction of CXCL2 (n=13), CXCL1 (n=13), and CXCL5 (n=23) was determined by quantitative PCR in the brains of WT mice with

EAE (grade 3+) compared to healthy control mice. Data are compiled from 4-5 independent experiments. **(e)** Fold induction of CXCL2 (WT, n=13; IL-17RA$^{-/-}$, n=6; IFN-γR$^{-/-}$, n=11), CXCL1 (WT, n=13; IL-17RA$^{-/-}$, n=6; IFN-γR$^{-/-}$, n=12), and CXCL5 (WT, n=21; IL-17RA$^{-/-}$, n=8; IFN-γR$^{-/-}$, n=9) was determined by quantitative PCR from brains of mice with EAE (grade 3+) compared to healthy control mice, and expressed as a percent of the induction seen in WT mice with EAE within the same experiment. Data are compiled from 2-3 independent experiments. NS, not significant; *** P<.001; **** P<.0001.

Neutrophil trafficking to the spinal cord is promoted by IFN-γ and does not require IL-17

Based on our observations that atypical but not classic EAE signs were decreased in IL-17RA$^{-/-}$ mice, and that inflammation in the brain correlated with neutrophil recruitment, we hypothesized that neutrophil recruitment to the spinal cord may not depend on IL-17 signaling. Consistent with this hypothesis, the absolute number of neutrophils was similar in the spinal cords of WT and IL-17RA$^{-/-}$ mice with EAE (**Fig. 3a**). Surprisingly, we found that neutrophil recruitment to the spinal cord was promoted by IFN-γ signaling as the number of neutrophils in the spinal cord was significantly reduced in IFN-γR$^{-/-}$compared to WT mice (**Fig. 3b**). Thus, IFN-γ signaling exerts opposite effects in the brain and spinal cord by promoting neutrophil recruitment to the spinal cord but inhibiting neutrophil influx into the brain. We then investigated whether expression of one or more ELR+ chemokines was induced via an IL-17-independent and IFN-γ-dependent mechanism. Expression of CXCL2 was of particular interest because CXCL2 was induced to a much greater extent than CXCL1 or CXCL5 in the spinal cord of WT mice with EAE (**Fig. 3c**), and its induction was more than 10-fold greater in the spinal cord compared to the brain (**Fig 2c and 3c**). We found that CXCL2 expression was induced to a comparable extent in the spinal cords of IL-17RA$^{-/-}$ and WT mice (**Fig. 3d**), confirming that an inflammatory mediator other than IL-17 can promote CXCL2 expression in the spinal cord. Importantly, CXCL2 induction was significantly decreased in the spinal cord of IFN-γR$^{-/-}$ mice compared to WT mice (**Fig. 3d**), indicating that IFN-γ signaling promotes CXCL2 induction in the spinal cord. The significant decrease in CXCL1 induction in IL-17RA$^{-/-}$ compared to WT spinal cords, coupled with the observation that neutrophil recruitment to the spinal cord was comparable in IL-17RA$^{-/-}$ and WT mice (**Fig. 3a, d**) suggested that CXCL1 does not contribute significantly to neutrophil recruitment to the spinal cord. Similarly, comparable CXCL5 induction in WT and IFN-γR$^{-/-}$

recipients did not correlate with the reduced neutrophil recruitment to IFN-γR$^{-/-}$ spinal cords (**Fig. 3b, d**). Thus, IFN-γ-dependent CXCL2 induction, rather than changes in expression of CXCL1 or CXCL5, correlated with IFN-γ dependent and IL-17-independent neutrophil recruitment to the spinal cord in mice with EAE.

To determine which cell types synthesize CXCL2 in the CNS during EAE, we sorted different cell subsets from CNS mononuclear cells isolated from mice at peak disease and analyzed induction of CXCL2 expression over cells sorted from healthy control mice using quantitative PCR. Astrocytes were the predominant source of CXCL2 induction in both the brain and spinal cord, and as observed for whole tissue, CXCL2 induction was much greater in spinal cord compared to brain astrocytes (**Fig. 4a**). Furthermore, CXCL2 induction was reduced in astrocytes isolated from the brain but not the spinal cord of IL-17RA$^{-/-}$ mice compared to WT mice (**Fig. 4b, c**), consistent with the notion that astrocytes are the primary producers of CXCL2 throughout the CNS during EAE.

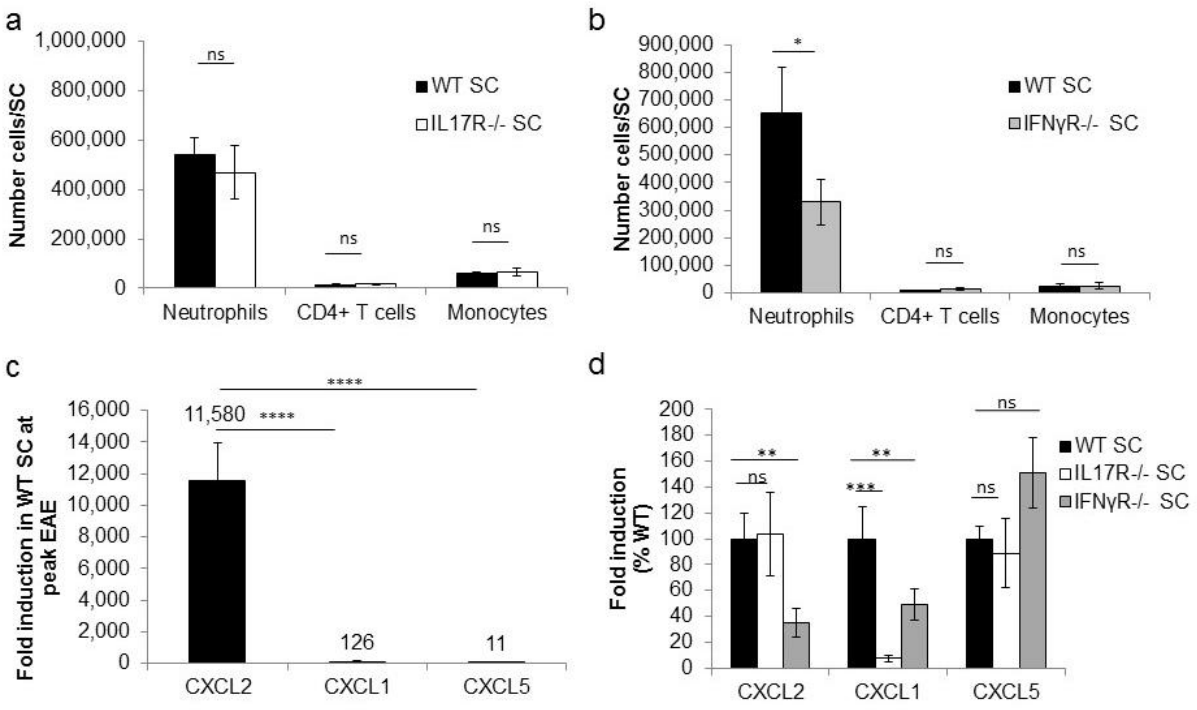

Figure 3. IFN-γ signaling promotes CXCL2 induction and neutrophil accumulation in the spinal cord. (a) The absolute number of neutrophils (WT, n=11; IL-17RA$^{-/-}$, n=6), CD4^{+} T cells (WT, n=11; IL-17RA$^{-/-}$, n=6), and inflammatory monocytes (WT, n=3; IL-17RA$^{-/-}$, n=3) are shown for cells isolated from the spinal cords (SC) of WT and IL-17RA$^{-/-}$ mice with EAE ≥ grade 3. Data are a compilation from 2-3 independent experiments. **(b)** The absolute number of neutrophils (WT, n=12; IFN-γR$^{-/-}$, n=13), CD4^{+} T cells (WT, n=8; IFN-γR$^{-/-}$, n=14), and inflammatory monocytes (WT, n=8; IFN-γR$^{-/-}$, n=10) are shown for cells isolated from the SC of WT and IFN-γR$^{-/-}$ mice with EAE ≥ grade 3. Data are compiled from 2-3 independent experiments. **(c)** Fold induction of CXCL2 (n=21), CXCL1 (n=13), and CXCL5 (n=24) as determined by quantitative PCR in the SC of WT mice with EAE compared to healthy control mice. Data are compiled from 4-5 independent experiments. **(d)** Fold induction of CXCL2 (WT, n=21; IL-17RA$^{-/-}$, n=8; IFN-γR$^{-/-}$, n=6), CXCL1 (WT, n=13; IL-17RA$^{-/-}$, n=4; IFN-γR$^{-/-}$, n=6) and CXCL5 (WT, n=24; IL-17RA$^{-/-}$, n=6; IFN-γR$^{-/-}$, n=6) was determined by quantitative PCR in

the SC of mice with EAE compared to healthy control mice, and expressed as a percent of the induction seen in WT mice with EAE within the same experiment. Data is a compiled from 2-3 independent experiments. NS, not significant; * P<.05; *** P<.001; **** P<.0001.

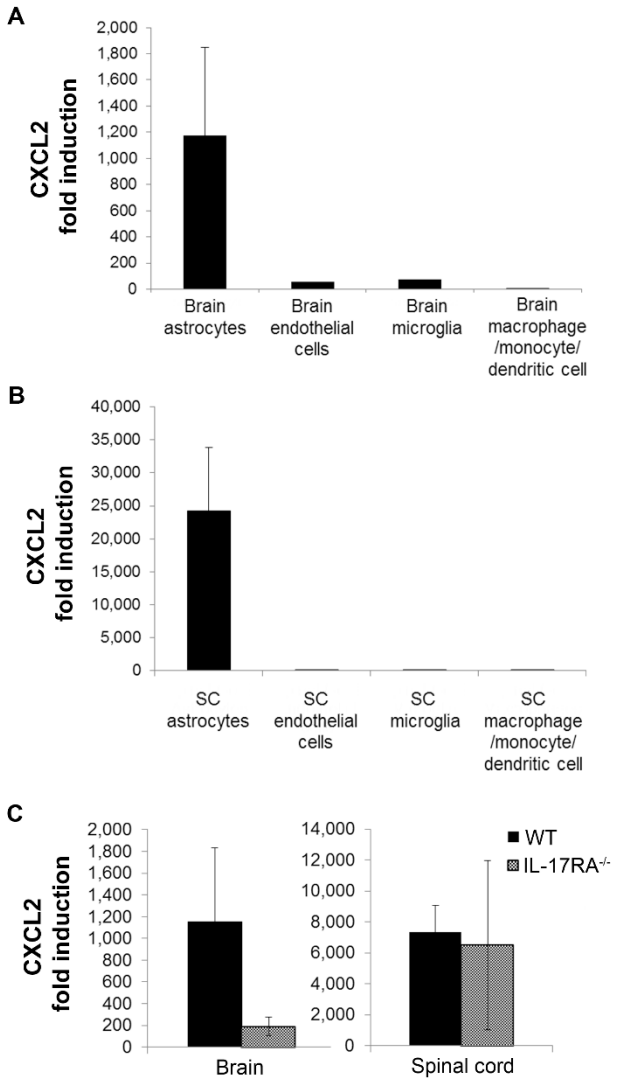

Figure 4. Astrocyte induction of CXCL2 is dependent on IL-17 signaling in the brain but not spinal cord. (A-B) Fold induction of CXCL2 compared to cells from naïve mice was determined by quantitative PCR for astrocytes ($CD45^{-}GFAP^{+}$), endothelial cells ($CD45^{-}CD31^{+}$), microglia ($CD45^{mid}CD11b^{+}$), and $CD45^{hi}CD11b^{+}$ cells sorted from the brains **(A)** and spinal cords (SC) **(B)** of WT mice with EAE ≥ 3. Data are compiled from 2 independent experiments with a total of 4 mice per group. **(C)** Fold induction of CXCL2 determined by quantitative PCR for astrocytes sorted from the brains and spinal cords of WT and IL-$17RA^{-/-}$ mice with EAE ≥ grade 3 compared to astrocytes sorted from healthy control brains. Data are compiled from 2

independent experiments, with 4 WT and 4 IL-17RA$^{-/-}$ brains and pooled samples from a total of 6 WT and 5 IL-17RA$^{-/-}$ spinal cords.

IFN-γ's differential effect in brain versus spinal cord tissue may depend on IL-1β induction and levels of IFN-γRα expression

The notion that IFN-γ signaling promotes CXCL2 induction by astrocytes was surprising as IFN-γ is more commonly known for inducing chemokines that attract monocytes [75, 76]. Therefore, we hypothesized that IFN-γ may induce CXCL2 indirectly, via induction of other inflammatory mediators. Previous *in vitro* studies have shown that IFN-γ signaling in bone marrow-derived macrophages can promote expression of IL-1β, a known inducer of ELR+ chemokines, under certain conditions [77]. We compared IL-1β expression in the brain and spinal cord of WT and IFN-γR$^{-/-}$ mice and found that, while no significant differences were observed in the brain, IL-1β expression was significantly decreased in the spinal cords of IFN-γR$^{-/-}$ compared to WT mice (**Fig. 5**), confirming that IFN-γ signaling promotes IL-1β expression in the spinal cord. In EAE, myeloid cells have been reported to be an important source of IL-1β [78]. We observed that in the myeloid lineage, both CD45^{hi}CD11b^{+} cells (including macrophages, monocytes, and dendritic cells) and microglia (CD45^{mid}CD11b^{+}) express IFN-γRα in the brain and spinal cord of naïve mice. Interestingly, however, CD45^{hi}CD11b^{+} cells isolated from the brain expressed a higher level of IFN-γRα compared to CD45^{hi}CD11b^{+} cells isolated from the spinal cord (an average median fluorescence intensity of 4425 versus 2050 in brain versus spinal cord macrophages respectively) (**Fig. 6a**), while the level of IFN-γRα expression did not differ between brain versus spinal cord microglia (**Fig. 6b**) or astrocytes (data not shown).[1] Therefore,

[1] These experiments were performed in triplicate on mice housed at UW. Similar experiments on mice housed at SLU did not show differing levels of IFN-γR in CD45^{hi}CD11b^{+} cells isolated from the brain and spinal cord. This may be due to differences in environmental factors resulting in changes to the microbiome.

varying levels of IFN-γRα expression in $CD45^{hi}CD11b^{+}$ cells may contribute to the differential response to IFN-γ in the brain compared to the spinal cord.

We hypothesized that differential levels of IFN-γRα may lead to induction of distinct downstream signaling pathways in macrophages in the brain compared to macrophages in the spinal cord. IFN-γ has been shown to induce a wide of variety downstream pathways by inducing phosphorylation of STAT-1; however, STAT-1 independent signaling pathways also exist. Therefore, I administered IFN-γ to cells isolated from brain versus spinal cord of naïve mice and assessed for phosphorylation of STAT-1 using flow cytometry. A preliminary experiment has suggested that $CD45^{hi}CD11b^{+}$ cells isolated from the brain may have increased levels of STAT-1 phosphorylation compared to $CD45^{hi}CD11b^{+}$ cells isolated from the spinal cord **(Fig. 7a)**; no difference in STAT-1 phosphorylation was observed for microglia isolated from brain compared to microglia isolated from spinal cord (**Fig. 7b**). This potential difference in STAT-1 phosphorylation between brain versus spinal cord $CD45^{hi}CD11b^{+}$ cells but not microglia correlates with differential levels of IFN-γRα expression in these cell types. Importantly, *in vitro* studies have shown that IFN-γ induces IL-1b in STAT-1-deficient macrophages, but not in WT macrophages [73], suggesting that IL-1b induction by macrophages occurs only in the absence of STAT-1 signaling. Therefore, if subsequent studies confirm that IFN-γ induces STAT-1 signaling in $CD45^{hi}CD11b^{+}$ cells isolated from brain but not spinal cord, it may account for the differential induction of IL-1β by IFN-γ in spinal cord and brain tissue during EAE.

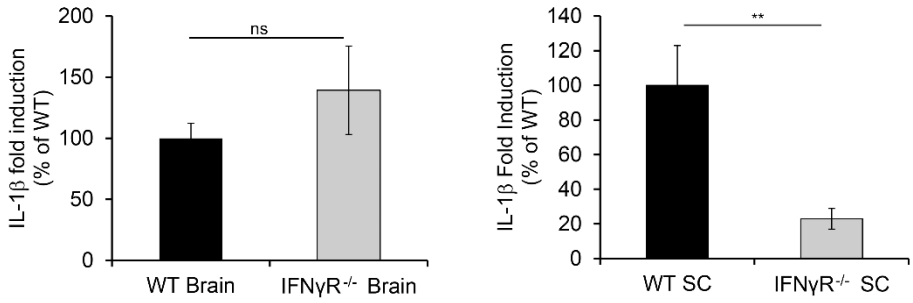

Figure 5. IFN-γ signaling promotes IL-1β in spinal cord but not brain tissue. Expression levels of IL-1β were determined by quantitative PCR for brain (left) and spinal cord (right) tissue harvested from WT (n=7) and IFN-$\gamma R^{-/-}$ (n=8) mice with EAE ≥ grade 3. Fold induction of IL-1β is shown for tissues from IFN-$\gamma R^{-/-}$ mice compared to healthy controls with expression of IL-1β in WT EAE mice assigned a value of 100%. Data are compiled from 2 independent experiments. NS, not significant; ** P<.01.

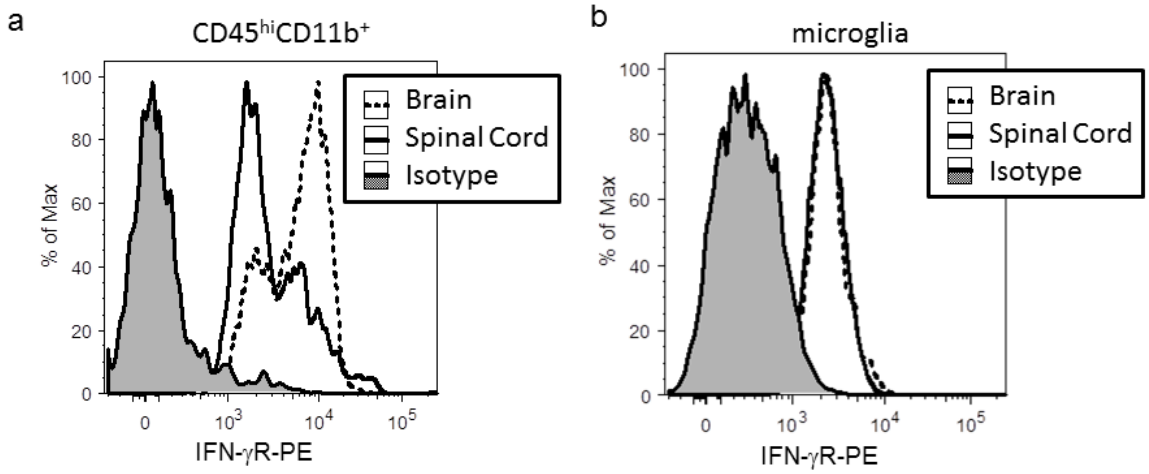

Figure 6. CD45^{hi}CD11b^{+} cells in the brain express higher levels of IFN-γRα than CD45^{hi}CD11b^{+} cells in the spinal cord. Cells were isolated from brains and spinal cords of naïve mice and stained for CD45, CD11b and either IFN-γRα or isotype control. Flow cytometric analyses of IFN-γRα expression is shown for CD45^{hi}CD11b^{+} cells **(a)** and CD45^{mid}CD11b^{+} microglia **(b).** Data are representative of 3 independent experiments.

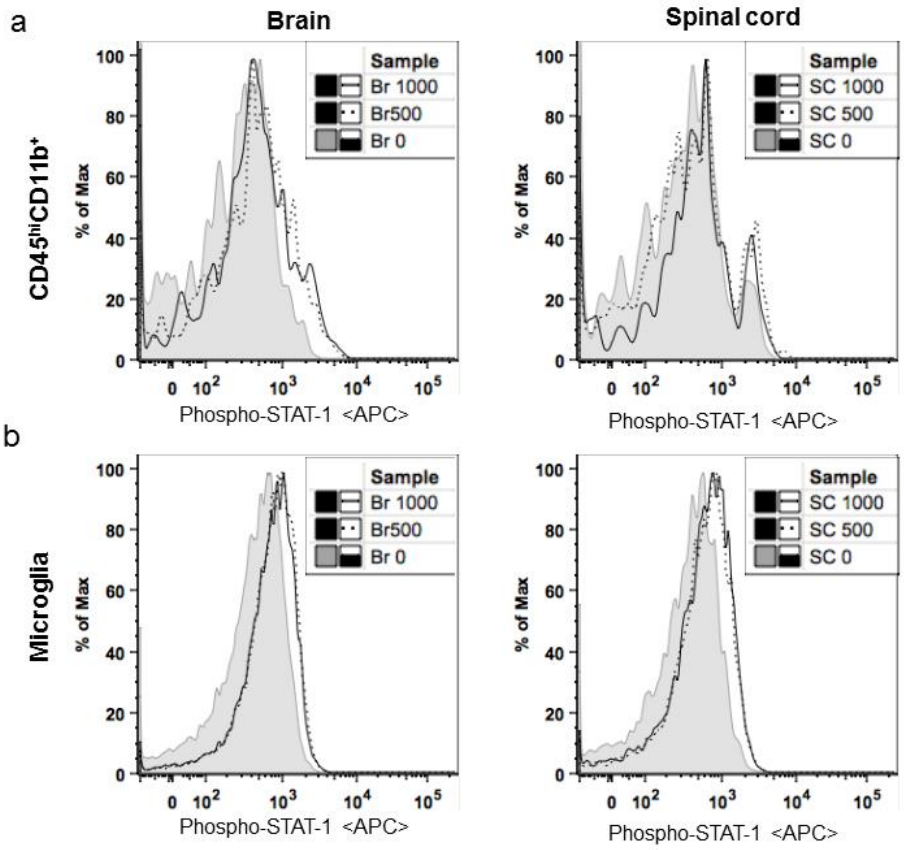

Figure 7. STAT-1 phosphorylation in response to IFN-γ may differ in brain versus spinal cord CD45^{hi} CD11b^{+} cells. Mononuclear cells isolated from collagenase-digested brains and spinal cords (SC) of naïve mice were incubated with rmIFN-γ (0, 500, and 1000 pg/mL). Phosphorylation of STAT-1 in response to rmIFN-γ is shown for CD45^{hi} CD11b^{+} cells **(a)** and CD45^{hi} CD11b^{low} microglia **(b).** Data is a single experiment from 3 pooled brain and 3 pooled spinal cords.

Chapter 4- ELR+ chemokine-mediated neutrophil recruitment is required for tissue injury in the brain, but not spinal cord during EAE

Neutrophil depletion suppresses more tissue injury in the brain than the spinal cord

Our finding that manifestation of clinical signs reflecting inflammation in the brain or spinal cord correlated with increased neutrophil recruitment to the particular CNS region led us to hypothesize that infiltrating neutrophils may play a critical role in promoting CNS tissue injury during EAE. To test this hypothesis, we depleted neutrophils by administering the neutrophil-specific anti-Ly6G antibody beginning on the day of CD4+ T cell transfer. The number of neutrophils, but not monocytes or lymphocytes, were significantly reduced in the blood of mice treated with anti-Ly6G (**Fig. 8a**). Interestingly, neutrophil depletion did not affect the overall incidence, onset, or severity of EAE (**Fig 8b**). Neutrophil depletion did, however, cause a dramatic change in the clinical manifestation of EAE. Neither the severity nor incidence (**Fig 8c, left**) of classic EAE signs was affected by neutrophil depletion. However, the incidence of atypical signs was drastically reduced in neutrophil-depleted mice compared to control mice (**Fig 8c, right**). To confirm that the absence of atypical signs reflected decreased tissue damage in the brain, we performed histopathological analyses of brain sections from neutrophil-depleted and control mice (**Fig. 9a, b**). The extent of inflammation in the brain was assessed by determining the area within each analyzed section that was populated by inflammatory foci. We observed a significant reduction in the percent area of brain sections containing lesions in mice treated with anti-Ly6G (**Fig 9c, left**). The extent of tissue damage was quantified by assigning a tissue injury score based on the extent of necrotic and apoptotic cell death associated with inflammatory lesions (as described in methods). There was a significant reduction in the tissue injury score for the brains of neutrophil-depleted versus control mice (**Fig 9c, middle**), consistent with the notion

that the absence of neutrophils is associated with less tissue damage in the brain. Strikingly, we also observed a pattern of pronounced perivascular cuffing in brain sections from neutrophil-depleted mice that was not commonly seen in comparable sections from control mice (**Fig. 9c, right**). Inflammatory cells consisting primarily of mononuclear cells localized around blood vessels without significant migration into the surrounding parenchyma in brain sections from neutrophil-depleted mice. In contrast, loss of vessel wall integrity was often observed in mice treated with isotype control antibody, and parenchymal brain tissue was heavily infiltrated by inflammatory cells with accompanying parenchymal tissue injury and occasional hemorrhage. Although the inflammatory cells in the brains of neutrophil-depleted mice did not appear to migrate as extensively into the parenchyma as in control mice, a diffuse pattern of gliosis was occasionally observed in the parenchyma of the anti-Ly6G treated-mice, which may reflect the activity of soluble inflammatory mediators. Overall, these findings suggest that neutrophils enhance the ability of inflammatory cells to migrate outside of the perivascular space surrounding blood vessels and subsequently promote parenchymal tissue injury.

The unexpected finding that classic EAE signs were still observed in neutrophil-depleted mice suggested that the spinal cord may be less dependent on neutrophil infiltration for tissue injury. We first confirmed that the neutrophil depletion protocol efficiently reduced the neutrophil number in the spinal cord, although the number of inflammatory monocytes was unchanged (**Fig. 10a**). Spinal cord sections were then analyzed for tissue injury as was performed with brain sections. The characteristics of spinal cord lesions were fundamentally similar to those seen in the brain in that isotype control-treated mice exhibited extensive parenchymal involvement and anti-Ly6G treated-mice demonstrated increased perivascular cuffing (**Fig 10b**). Quantitative analyses showed a decrease in percent area populated by

inflammatory cells (**Fig. 10c, left**), and an increase in the number of perivascular cuffs (**Fig. 10c, right**) in spinal cord sections from neutrophil-depleted mice compared to control mice. A decrease in tissue injury was observed in the spinal cords of neutrophil-depleted mice (**Fig. 10c, middle**), however, the decrease was less than that observed in the brains of these mice (**Fig. 9c, middle**). These data suggest that the loss of atypical but not classic EAE signs in neutrophil-depleted mice may reflect a greater role for neutrophils in mediating tissue damage in the brain compared to the spinal cord.

a

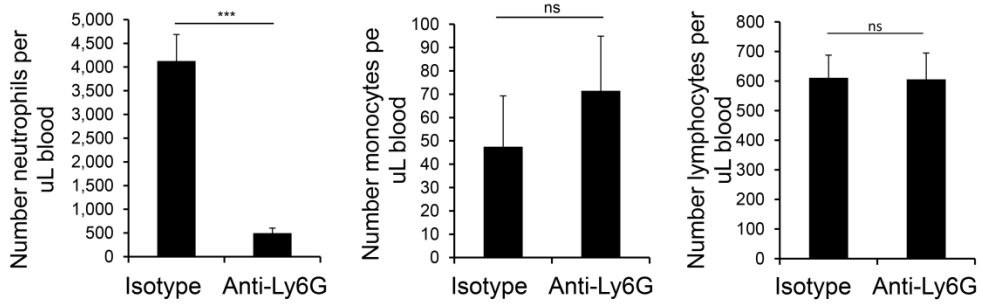

b

	Isotype treated	Anti-Ly6G treated	P-value
Overall EAE incidence	96% (22/23)	96% (24/25)	ns
Peak EAE score	5.1	4.9	ns
Day of onset	6.7	6.8	ns

c

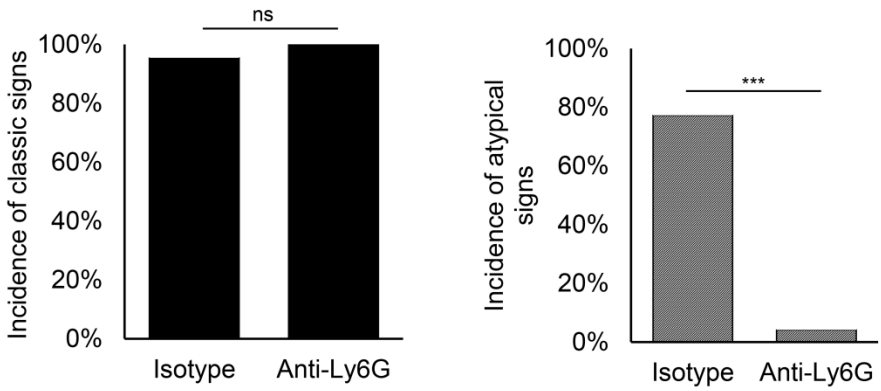

Figure 8. Atypical EAE is dependent on neutrophil infiltration. (a) The absolute number of neutrophils (left), monocytes (middle), and lymphocytes (right) per microliter (uL) blood as assessed by CBC with differential is shown for isotype-treated (n=8) and anti-Ly6G-treated (n=8) mice. **(b)** Clinical data from WT mice treated with anti-Ly6G or isotype control antibody are shown. Peak EAE score and clinical onset were calculated from mice that succumbed to EAE (isotype-treated, n=22; anti-Ly6G-treated, n=24). Data are compiled from 5 independent experiments. **(c, left)** Incidence of classic EAE signs expressed as a percentage of sick mice, with or without accompanying atypical EAE signs in mice shown in (a). **(c, right)** Incidence of

atypical EAE signs expressed as a percentage of sick mice, with or without accompanying classic signs, in mice shown in (a). NS, not significant; *** P<.001.

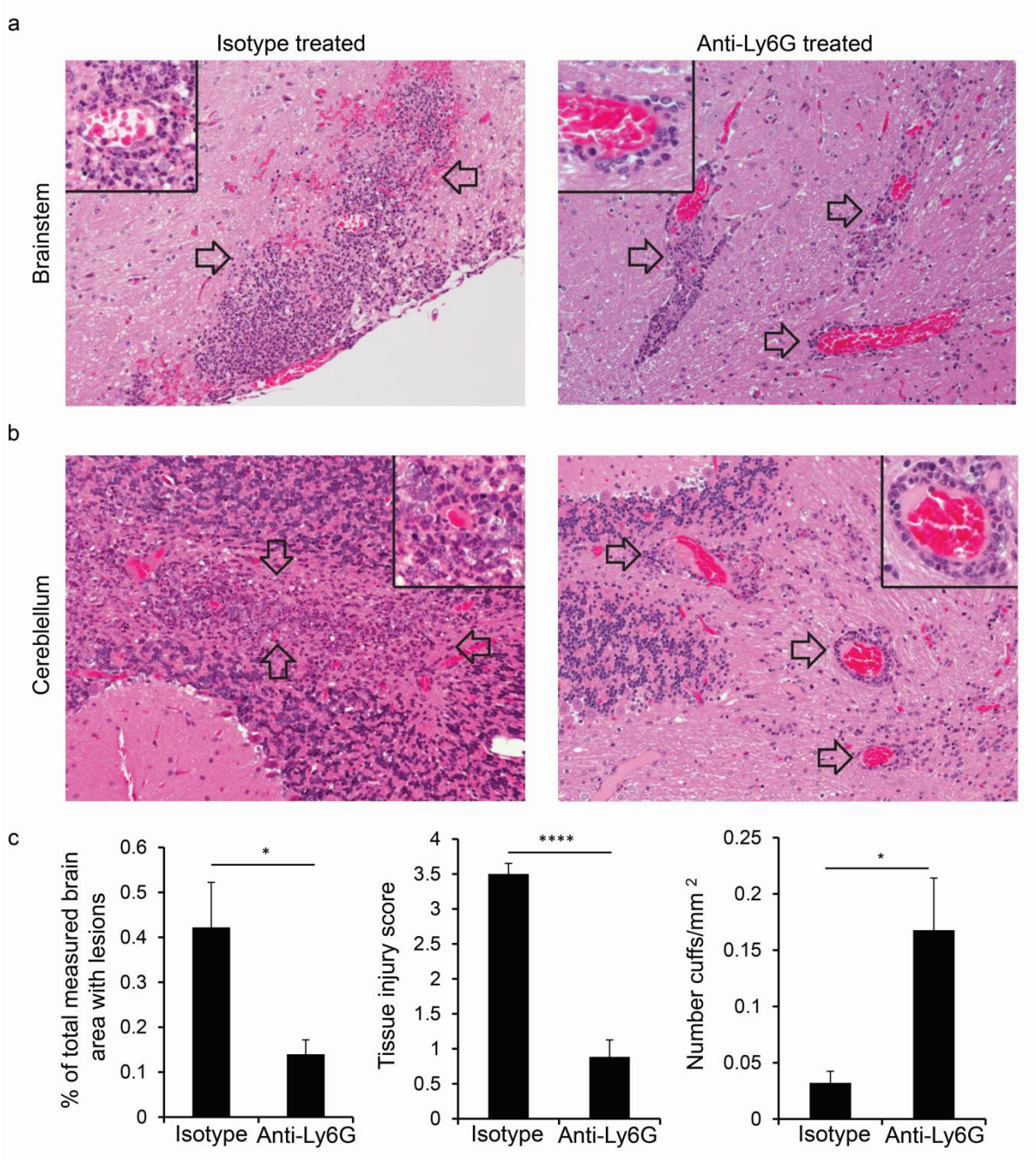

Figure 9. Tissue damage in the brain requires neutrophil infiltration. (a,b) Histopathology is shown for representative sections from brainstem (**a**) and cerebellum (**b**) from WT mice treated with isotype control (left) or anti-Ly6G antibody (right) with EAE ≥ grade 3. Images (20X) are representative of 12 isotype control-treated and 13 anti-Ly6G-treated mice from 3 independent experiments. Focally extensive highly cellular inflammatory lesions (arrows) predominate in

white matter of control animals (left); insets (60X) reveal dense accumulation of neutrophils admixed with fewer mononuclear cells as well as necrotic and apoptotic cell debris in lesions. In contrast, lesions within similar white matter regions of anti-Ly6G-treated mice (right) lack the obvious extended parenchymal involvement seen in control mice. These lesions have a more localized perivascular signature (arrows) comprised predominantly of mononuclear cells and are associated with a much diminished necrotic change (inset). (**c**) Analyses of brain sections from 12 isotype control-treated and 13 anti-ly6G-treated mice with EAE ≥ 3 are shown quantifying the total brain sectional area affected with lesions (left), the severity of tissue injury (middle), and the prevalence of perivascular cuffing (right). Data are compiled from 3 independent experiments. * P<.05; **** P<.0001

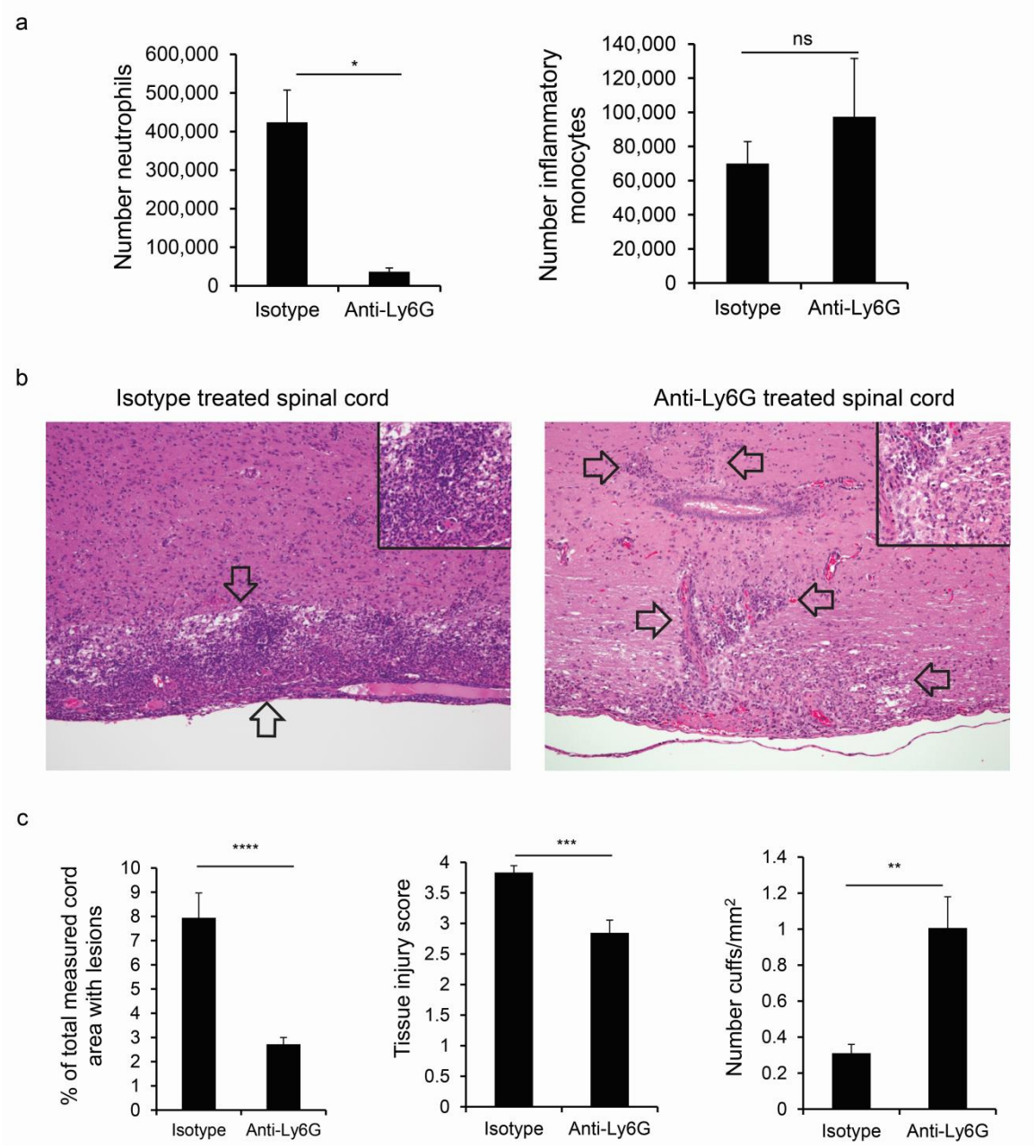

Figure 10. Tissue damage in the spinal cord is less dependent on neutrophils than the brain.

(a) The absolute number of neutrophils ($CD45^+CD11b^+Ly6C^{int}$, left) and inflammatory monocytes ($CD45^+CD11b^+Ly6C^{hi}$, middle) assessed by flow cytometry are shown for spinal cords of isotype-treated (n=4) and anti-Ly6G-treated (n=4) mice. **(b**) Histopathology is shown for representative spinal cords from WT mice treated with isotype control (left) or anti-Ly6G

antibody (right). Images (10X) are representative of 12 isotype control-treated and 13 anti-Ly6G-treated mice from 3 independent experiments. Focally extensive highly cellular inflammatory lesions (between arrows) predominate in control animals (left); inset (60X) reveals dense accumulation of neutrophils admixed with fewer mononuclear cells as well as necrotic and apoptotic cell debris in lesions. In spinal cords of anti-Ly6G-treated mice (right), mononuclear cells surround vessels or are present as focal accumulations (arrows); lesions are associated with some necrotic and apoptotic cell debris and are comprised predominantly of mononuclear cells (inset; 60X). **(c)** Analyses of spinal cord (SC) sections from 12 isotype control-treated and 13 anti-ly6G-treated mice with EAE ≥ 3 are shown quantifying the total spinal cord sectional area affected with lesions (left), the severity of tissue injury (middle), and the prevalence of perivascular cuffing (right). Data are compiled from 3 independent experiments. ** P<.01; *** P<.001; **** P<.0001.

CXCR2 antagonism is therapeutically equivalent to neutrophil depletion

The results described above suggested that preventing neutrophil infiltration during CNS autoimmunity prevented clinical signs associated with tissue damage in the brain but not the spinal cord. As neutrophil recruitment correlated with induction of the ELR+ chemokine CXCL2, we investigated whether blocking ELR+ chemokine signaling *in vivo* would recapitulate the therapeutic effect of neutrophil depletion on atypical EAE. A small molecule antagonist of CXCR2, the main receptor for ELR+ chemokines on neutrophils, was administered daily beginning on the day of T cell transfer. As observed for neutrophil-depleted mice, the onset, peak severity, and incidence of classic EAE signs were similar between mice that received the CXCR2 antagonist and control mice. However, the incidence of atypical signs was reduced from 73% in mice treated with vehicle control to zero in antagonist-treated mice (**Fig. 11a-c**). These striking data show that antagonizing CXCR2 signaling *in vivo* during EAE is therapeutically equivalent to neutrophil depletion in preventing clinical signs of brain inflammation. Interestingly, CXCR2 antagonism did not lead to a reduction in neutrophil numbers by flow cytometry (**Fig. 12a**). There is some evidence, however, that CXCR2 antagonism may change the localization of neutrophils, as some mice treated with the CXCR2 antagonist showed neutrophils retained in the perivascular space by H&E (**Fig. 12b**) instead of spreading deeply into tissue parenchyma as seen in WT mice (**Fig. 9a**). More H&E studies need to be performed, however, before definitive conclusions can be made regarding the effects of CXCR2 antagonism on neutrophil localization.

a

	H_20 treated	CXCR2 antagonist treated	P-value
Overall EAE incidence	92% (12/13)	90% (10/11)	ns
Peak EAE score	3.5	3.0	ns
Day of onset	6.7	6.8	ns

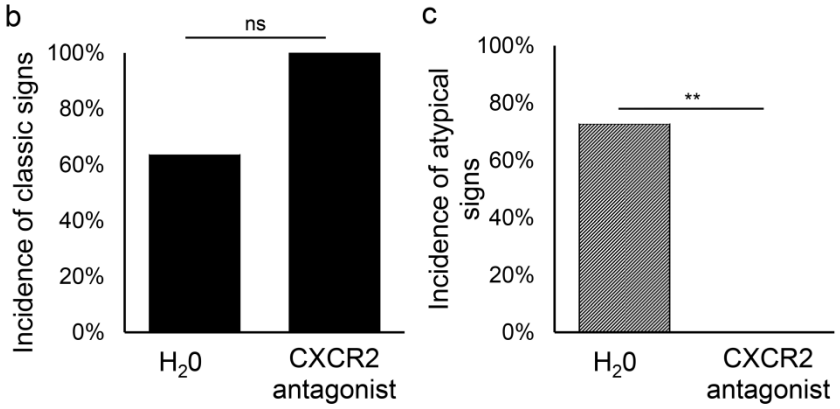

Figure 11. Atypical EAE requires CXCR2 signaling. (a) Clinical data from WT mice treated with CXCR2 antagonist or vehicle control (H_20) are shown. Peak EAE score and clinical onset were calculated from mice that succumbed to EAE (control, n=12; CXCR2 antagonist-treated, n=10). Data are compiled from 2 independent experiments. **(b)** Incidence of classic EAE signs expressed as a percentage of sick mice, with or without accompanying atypical EAE signs in mice shown in (a). **(c)** Incidence of atypical EAE signs expressed as a percentage of sick mice, with or without accompanying classic EAE signs, in mice shown in (a). NS, not significant; ** P<.01.

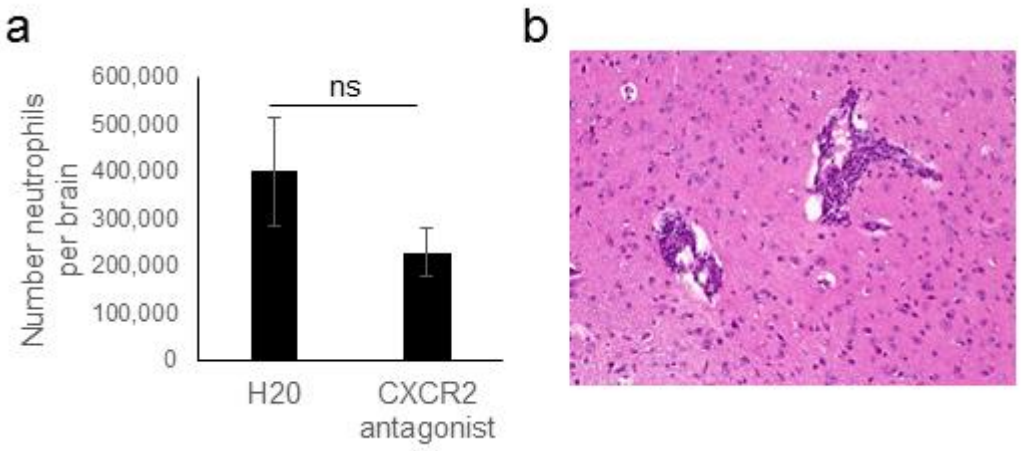

Figure 12. CXCR2 antagonism may change the localization, but not number of neutrophils in the brain. (a) The number of neutrophils ($CD11b^{+}Ly6G^{+}$) was assessed using flow cytometry in the brains of control (n=12) and CXCR2 antagonist-treated (n=11) mice. **(b)** H&E image is shown from the brain of a CXCR2 antagonist treated mouse. *NS, not significant.*

Neutrophil depletion inhibits classic and atypical disease in IFN-γR$^{-/-}$ mice

As demonstrated above, IFN-γ signaling strongly inhibits neutrophil recruitment to the brain and development of atypical EAE signs in WT mice. To investigate whether the increased incidence of atypical signs seen in IFN-γR$^{-/-}$ mice was due to enhanced neutrophil infiltration to the brain, we induced EAE by adoptive transfer in IFN-γR$^{-/-}$ mice and treated daily with the neutrophil depleting antibody anti-Ly6G or isotype control. Overall EAE incidence was greatly reduced in IFN-γR$^{-/-}$ mice treated with anti-Ly6G (**Fig. 13a**), suggesting that neutrophils contribute to the development of overall inflammation throughout the CNS in these mice. However, of those IFN-γR$^{-/-}$ mice that developed EAE, there was a drastic reduction in the incidence of atypical clinical signs (86% versus 14% in control versus anti-Ly6G-treated mice, respectively, **Fig. 13b**), but no reduction in the incidence of classic signs (86% versus 100% in control versus anti-Ly6G-treated mice, respectively, **Fig. 13b**). These findings demonstrated that atypical EAE in IFN-γR$^{-/-}$ mice requires neutrophils, and suggested that neutrophil depletion has a larger impact in the brain compared to the spinal cord.

a

	Isotype-treated	Anti-Ly6G-treated
Overall EAE incidence	85.7% (6/7)	42.9% (3/7)
Peak EAE score	3.8	4.7
Day of onset	10.0	11.7

b

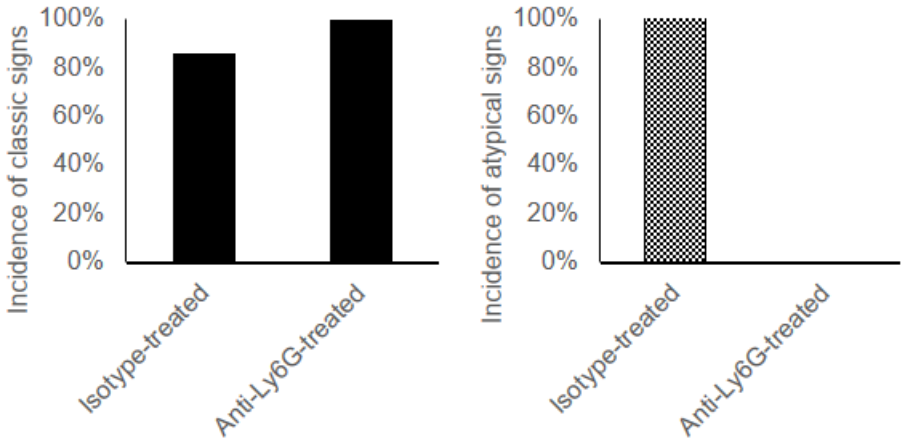

Figure 13. Neutrophil depletion ameliorates atypical signs and reduces overall EAE incidence in IFN-γR$^{-/-}$ mice. (a) Clinical data from IFN-γR$^{-/-}$ mice treated with anti-Ly6G (n=7) or isotype control (n=7) antibody are shown. Peak EAE score and clinical onset were calculated from mice that succumbed to EAE (anti-Ly6G, n=3; isotype, n=6). Data are from a single experiment. **(b)** Incidence of classic EAE signs expressed as a percentage of sick mice, with or without accompanying atypical EAE signs in mice shown in (a). **(c)** Incidence of atypical EAE signs expressed as a percentage of sick mice, with or without accompanying classic EAE signs, in mice shown in (a).

Chapter 5- Atypical EAE can develop in the absence of IL-17 signaling when neutrophils are recruited to the brain

Development of atypical EAE following active EAE induction is less dependent on IL-17 signaling

The studies described in chapters 2 and 3 above were performed using passive EAE induction, in which EAE is induced by the transfer of T_H17-skewed myelin-specific T cells. We have also investigated the role of IL-17 signaling in atypical EAE following active EAE induction and have observed mixed results. In initial experiments, WT and IL-17RA$^{-/-}$ mice developed atypical EAE signs with similar incidence and severity (**Fig. 14a**), and pathology demonstrated that the severity of brain inflammation did not differ between WT and IL-17RA$^{-/-}$ mice in the cortex, cerebellum, or brainstem (**Fig. 14b**). These data suggested that atypical EAE and brain inflammation following active EAE induction was not dependent on IL-17 signaling. Because neutrophils were found to be required for atypical EAE signs in the passive EAE induction model (described in chapter 3), we hypothesized that following active immunization, neutrophils are recruited to the brain in an IL-17-independent manner, leading to the development of atypical EAE signs in IL-17RA$^{-/-}$ mice. Consistent with this hypothesis, we found that WT and IL-17RA$^{-/-}$ mice with actively-induced EAE had similar neutrophil numbers in the brain (**Fig. 14c**). These data showed that following active EAE induction, neutrophil accumulation in the brain correlates with atypical EAE signs, even in the absence of IL-17 signaling.

Interestingly, over time I saw a shift in the role of IL-17 signaling in atypical EAE development following active EAE induction. In subsequent experiments, IL-17RA$^{-/-}$ mice with actively-induced EAE had a much lower incidence of atypical EAE signs than their WT

counterparts. It is not clear why actively-induced EAE changed in our colony over time. It is possible that changes in the pertussis toxin or rMOG used for disease induction influenced the manifestation of EAE in these mice. This data suggests that in some instances, atypical EAE can proceed in the absence of IL-17 signaling. I hypothesize that this IL-17-independent atypical EAE correlates with IL-17-independent neutrophil accumulation in the brain

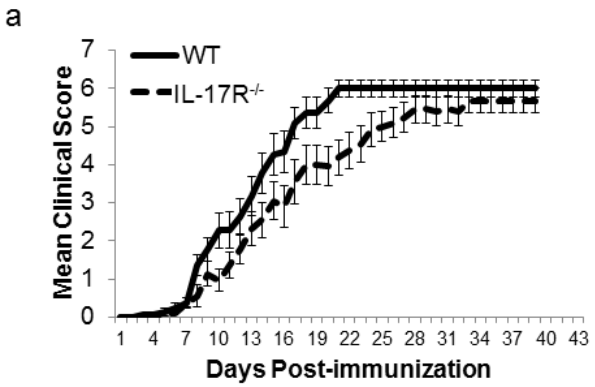

	WT	IL-17R$^{-/-}$
Overall EAE Incidence	100% (22/22)	100% (23/23)
Peak EAE score	6	5.7
Incidence of atypical signs	100% (22/22)	100% (23/23)

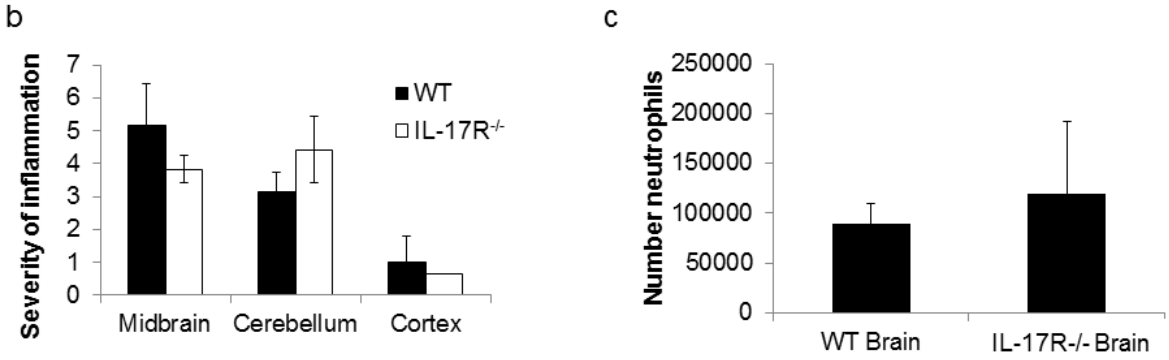

Figure 14. Atypical EAE and neutrophil recruitment to the brain occurs independent of IL-17 signaling following active EAE induction. (a) Clinical data from WT (n=22) and IL-17RA$^{-/-}$ (n=23) mice following active EAE induction. **(b)** Severity of inflammation in midbrain, cerebellum, and cortex was determined from H&E slides from same mice in (A). **(c)** Number of neutrophils in the brains of WT (n=4) and IL-17RA-/- (n=4) mice was determined by flow cytometry upon development of grade ≥ 3 following active EAE induction.

Development of atypical EAE following adoptive transfer of IL-17RA$^{-/-}$ T cells is not dependent on host IL-17 signaling

Based on the observations in early experiments that IL-17RA$^{-/-}$ mice develop more atypical EAE following active induction (immunization) than following passive induction (transfer of WT T cells), I sought to understand what accounted for the different outcomes following these two methods of EAE induction. During active EAE induction in IL-17RA$^{-/-}$ mice, myelin-specific T cells thought to be responsible for triggering disease are derived from host IL-17RA$^{-/-}$ mice, while in the passive EAE induction described above, myelin-specific T cells derived from WT mice (IL-17RA$^{+/+}$) are transferred into IL-17RA$^{-/-}$ hosts. Therefore, I hypothesized that expression of IL-17RA on CD4^{+} T cells may account for the increased atypical signs seen in IL-17RA$^{-/-}$ mice during active versus passive EAE induction. In order to test this hypothesis, I induced EAE by transferring either WT CD4^{+} T cells or IL-17RA$^{-/-}$ CD4^{+} T cells into IL-17RA$^{-/-}$ hosts and observed mice for development of atypical EAE signs. I found that IL-17RA$^{-/-}$ hosts had a higher incidence of atypical EAE signs following transfer of IL-17RA$^{-/-}$ T cells than following transfer of WT T cells (60% versus 9% following transfer of IL-17RA$^{-/-}$ versus WT T cells, respectively, **Fig. 15a, left panel**). Consistent with an important role for neutrophils in atypical EAE, I also observed increased neutrophil accumulation in the brains of IL-17RA$^{-/-}$ mice following the transfer of IL-17RA$^{-/-}$ T cells versus WT T cells (**Fig. 15b**), although neutrophil numbers were not increased to the full levels seen in WT mice that had received WT T cells. There was also a trend towards increased CXCL2 induction in the brains of IL-17RA$^{-/-}$ hosts receiving IL-17RA$^{-/-}$ T cells compared to WT T cells (**Fig. 15c**), consistent with an important role for ELR+ chemokines in neutrophil recruitment to the brain and atypical EAE. I hypothesized that the differences in CXCL2 induction and neutrophil recruitment in recipients of

WT and IL-17RA$^{-/-}$ T cells may be due to differences in cytokine production by WT and IL-17RA$^{-/-}$ T cells, and therefore assessed IL-17RA$^{-/-}$ and WT T cells for cytokine production on the day of adoptive transfer. I found no significant difference in IL-17, IFN-γ, or GM-CSF production by ELISpot on the day of adoptive transfer. However, it is possible that these cells may be reactivated differently in IL-17RA$^{-/-}$ hosts and therefore, investigating cytokine production at pre-clinical and clinical timepoints *ex vivo* may reveal important differences between these T cells.

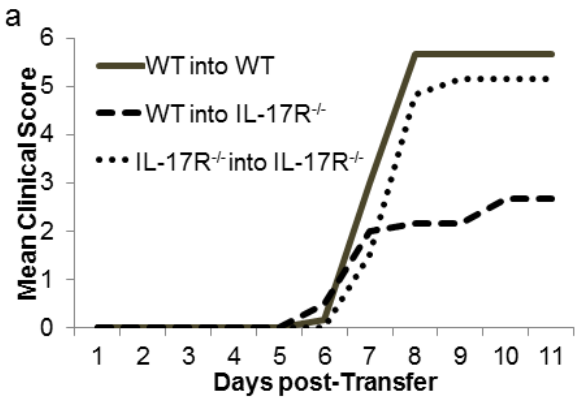

	WT into WT	WT into IL-17R$^{-/-}$	IL-17R$^{-/-}$ into IL-17R$^{-/-}$
Overall EAE Incidence	100% (17/17)	61% (11/18)	88% (15/17)
Peak EAE score	5.7	3.1	5.2
Incidence of atypical signs	53% (9/17)	9% (1/11)	60% (9/15)

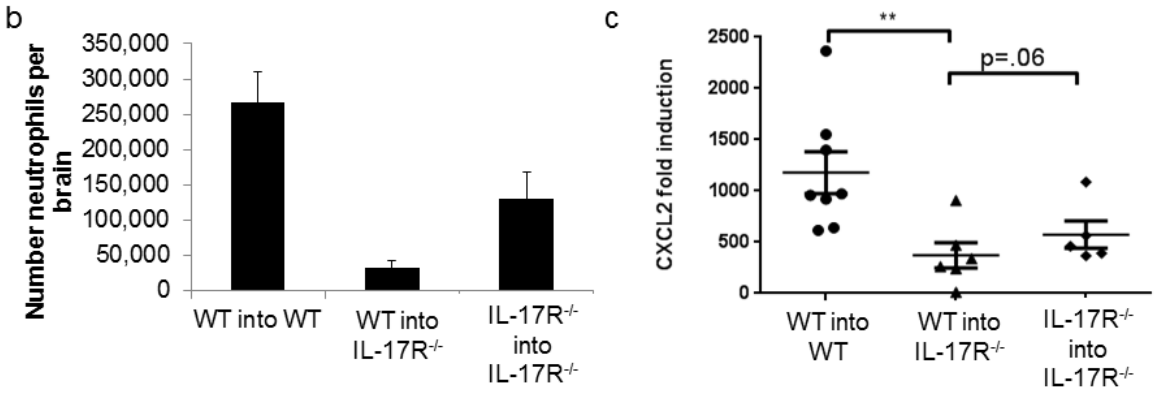

Figure 15. Atypical EAE develops in IL-17RA$^{-/-}$ hosts following transfer of IL-17RA-/- T cells. (a) Clinical data from mice following transfer of WT T cells in WT (n=17) and IL-17RA-/- (n=18) hosts and IL-17RA$^{-/-}$ T cells into IL-17RA$^{-/-}$ hosts (n=17). Peak EAE score and incidence of atypical signs was calculated for mice that succumbed to EAE. **(b)** Number of neutrophils in the brain was determined by flow cytometry for mice from (a). **(c)** Fold induction of CXCL2 was determined in the brains of mice from (a) with a grade ≥3 compared to brains of naïve mice. **, P<.01.

Chapter 6- Concluding Remarks and Remaining Questions

The mechanisms that direct inflammatory cells to localize within specific CNS regions in patients with MS have been poorly understood. Clinically, this is a critical question because the location of lesions within the CNS determines the clinical signs seen in individual patients, which in turn influences the extent of their disability. Our studies in EAE investigating the role of IL-17 and IFN-γ provide important insight into this question. We found that the development of EAE was strongly impaired in mice simultaneously deficient in both IL-17 and IFN-γ signaling, but that the brain and spinal cord function as distinct microenvironments with respect to their response to each of these cytokines. In the brain, IL-17 is the driving force underlying ELR+ chemokine induction and neutrophil recruitment following adoptive transfer of WT IL-23 skewed cells, while IFN-γ appears to inhibit this pathway. Importantly, we showed that neutrophil infiltration plays a critical role in promoting tissue injury in the brain during disease onset and is required for the development of atypical clinical signs. Also of note, in some instances such as active EAE induction and following transfer of IL-17RA$^{-/-}$ T cells, neutrophil accumulation to the brain can proceed in the absence of IL-17 signaling. When this occurs, atypical EAE and parenchymal brain lesions can develop. In the spinal cord, we observed that surprisingly, IFN-γ rather than IL-17 plays the major role in recruiting neutrophils following adoptive transfer of WT IL-23 skewed cells. However, while neutrophils contribute to tissue injury in the spinal cord, tissue injury in this microenvironment appears less dependent on neutrophils compared to the brain as neither the incidence nor severity of classic EAE signs were reduced following antibody-mediated neutrophil depletion *in vivo*. Together these findings reveal pronounced differences between the brain and spinal cord in their response to inflammatory stimuli and their sensitivity to mediators of tissue damage.

Identifying mechanisms that promote lesion formation in the brain parenchyma is especially relevant to patients with MS, the majority of whom have lesions in this region. Earlier studies demonstrated that IFN-γ produced by T_H1 cells inhibited lesion formation in the brain and atypical EAE signs [61, 62, 69, 79]. In mice deficient in IFN-γ or IFN-γR signaling, the inflammatory infiltrate in the brain during EAE was often dominated by neutrophils [61, 69]. Subsequently, our laboratory and others demonstrated that T_H17 cells and IL-17 signaling preferentially promoted brain inflammation [58, 59, 80]. While IL-17 is known to induce ELR+ chemokine induction and neutrophil recruitment in a wide variety of inflammatory settings, it was not known whether this activity was actually responsible for the ability of IL-17 to promote brain inflammation. Here we established the functional significance of IL-17-mediated neutrophil recruitment by demonstrating that neutrophil recruitment to the brain is required for the development of atypical EAE. Our data also provide a mechanistic basis for the antagonistic effects of IL-17 and IFN-γ in the development of atypical EAE. Our results indicate that the "cross-talk" between IL-17 and IFN-γ in regulating lesion formation in the brain arises from the ability of each cytokine to regulate, in an opposing fashion, ELR+ chemokine induction and neutrophil recruitment in this microenvironment. Neutrophils were required to promote the disseminated leukocyte infiltration that leads to severe tissue damage in the brain and atypical clinical signs. In the absence of neutrophils, inflammatory cells were largely retained in perivascular spaces, resulting in only mild gliosis in the surrounding brain tissue. This is consistent with other work suggesting that neutrophils enhance blood-brain-barrier permeability [81] and promote the invasion of immune cells deep into tissue parenchyma [69, 82]. Taken together, our data indicate that atypical EAE is regulated by the opposing pathways triggered by IL-17 and IFN-γ that modulate expression of ELR+ chemokines, particularly CXCL2. The

importance of ELR+ chemokine expression in regulating brain inflammation was confirmed by the complete loss of atypical EAE observed in mice treated with an antagonist of CXCR2, a receptor for ELR+ chemokines that is expressed on neutrophils. We have also shown that when neutrophil recruitment to the brain proceeds in an IL-17-independent manner (such as following transfer of IL-17RA$^{-/-}$ T cells or sometimes following active EAE induction), parenchymal brain inflammation can still develop.

Our finding that IFN-γ, rather than IL-17 signaling, promoted CXCL2 induction and neutrophil recruitment in the spinal cord was surprising and highlights the differences in immunoregulation within the distinct microenviroments of brain and spinal cord tissue. We found that astrocytes were the predominant producers of CXCL2 in the brain and spinal cord during EAE, and that the differential effect of IL-17 signaling on CXCL2 production that we observed in brain compared to spinal cord tissue was also observed for astrocytes sorted from these tissues and analyzed directly *ex vivo*. However, the pathways that result in differential production of CXCL2 by astrocytes in the brain versus the spinal cord are not known, and other cell types and mediators may be involved that are downstream of IFN-γ signaling in the spinal cord. For example, IFN-γ signaling in the spinal cord significantly promoted induction of IL-1β, a known inducer of ELR+ chemokines. Therefore, IFN-γ-mediated induction of CXCL2 in the spinal cord could be a consequence of increased expression of IL-1β, which in turn elicits CXCL2 production from astrocytes. In contrast, IFN-γ signaling did not promote IL-1β in the brain. Further studies are warranted to define the inflammatory mediators and their cellular targets that ultimately lead to differential production of CXCL2 by astrocytes and how these differ in the brain versus the spinal cord.

In light of the dependence of CXCL2 expression on IFN-γ signaling in the spinal cord, it was not surprising that neutrophil recruitment and incidence of classic EAE signs was promoted by IFN-γ signaling in this region. However, we were surprised to find that depleting neutrophils did not impair development of classic EAE in our model. Some tissue damage in the spinal cord was ameliorated by neutrophil depletion, but the protection from tissue injury was not equivalent to that observed in the brain. It is possible that the small number of neutrophils that remain following treatment with anti-Ly6G is sufficient to induce injury in the more contained microenvironment of the spinal cord. Alternatively, the spinal cord may be more sensitive to injury mediated by other cell types compared to the brain microenvironment. Although atypical EAE signs were abolished by treatment with a CXCR2 antagonist, 100% of these mice still developed classic EAE. This observation supports the notion that other inflammatory cells recruited via a CXCR2-independent mechanism may mediate spinal cord injury in this model without a requirement for neutrophil infiltration. The contribution of neutrophils to spinal cord injury, however, may vary depending on the mouse strain, phenotype of effector cells inducing disease, and mode of induction [58, 81].

Defining requirements for spinal cord inflammation during CNS autoimmunity has been complex as there are a number of conflicting reports on the roles of cytokines in classic EAE models. IL-17 signaling was shown to be important in some [54-57], but not all [58-60] models of classic EAE. Likewise, IFN-γ has been shown to promote spinal cord inflammation in some [61, 62, 83], but not all [58, 82] classic EAE models. Recently, several studies suggested that GM-CSF, rather than IL-17 or IFN-γ, is required for spinal cord inflammation [58, 84-87]. It is possible that these differing results reflect differences in EAE models and/or that more diverse inflammatory stimuli can induce inflammation in the spinal cord compared to the brain. This

latter notion is consistent with our previous report that inflammation in the brain requires a Th17:Th1 ratio >1, while the spinal cord is susceptible to inflammation induced by a wide range of Th17:Th1 ratios. It is also consistent with our current findings that, while CXCR2-dependent neutrophil recruitment is required for parenchymal tissue injury in the brain, it may be redundant with the activity of other cell types capable of promoting parenchymal tissue damage in the spinal cord.

Consistent with the mechanisms we identified in regulating brain inflammation in EAE, there is evidence supporting a role for the IL-17-induced ELR+ chemokine pathway in patients with MS, the majority of whom have lesions located throughout the brain parenchyma. IL-17 transcripts are highly expressed in lesions [88], as well as blood and CSF mononuclear cells of patients with MS [89]. In addition, protein levels of CXCL8, the human ortholog for CXCL1 and CXCL2, are increased in the CSF of patients with MS [90]. Importantly, early phase IIa clinical trials indicated that treatment with secukinumab, a monoclonal antibody directed against IL-17A, resulted in a reduction in inflammatory lesions in the brain and a trend towards reduced clinical relapses in patients with MS compared to placebo-treated controls [91]. However, a role for neutrophils in MS has been controversial because they are not often found in CNS tissue obtained either post-mortem or by biopsy from patients with MS. Notably, our data support a role for neutrophils during lesion formation in the acute phase of CNS autoimmunity, while tissue sections from MS patients are typically analyzed long after disease onset. The observation that pediatric MS patients with earlier onset have a higher proportion of neutrophils in the CSF compared to patients with later onset supports the notion that neutrophils may be most important during the initial stages of disease. In these patients, the proportion of neutrophils in the CSF decreases with increasing disease duration, while the proportion of lymphocytes and monocytes

increases [92]. Our studies suggest that neutrophils could be most relevant during the early stages of MS by facilitating the initial leukocyte trafficking from the perivascular space into the brain parenchyma. A role for neutrophils in chronic disease, however, is also suggested by the observation that neutrophils in the blood of patients with MS exhibit a primed phenotype compared to healthy controls and that neutrophil numbers increase during disease relapse [93]. In addition, treatment with rhG-CSF, which supports neutrophil activation, worsens the clinical status in patients with MS [94], and neutrophil depletion in a relapsing-remitting EAE model inhibited relapses [81]. Together these observations suggest that neutrophils may play a more important role in the pathogenesis of MS than previously appreciated.

In conclusion, our studies show that IL-17 and IFN-γ regulate the development of atypical EAE and tissue injury in the brain via their opposing effects on ELR+ chemokine-mediated neutrophil infiltration into the brain parenchyma, which is required for the development of brain lesions. Therefore, disruption of ELR+ chemokine-mediated neutrophil recruitment may be effective in preventing development of brain lesions in patients with MS. Our data also show that cytokines produced by infiltrating T cells trigger very distinct immune responses triggered in the brain compared to the spinal cord, indicating that the predominant site of lesion activity in a patient should be considered in designing effective therapies.

Chapter 7- Supplemental Data

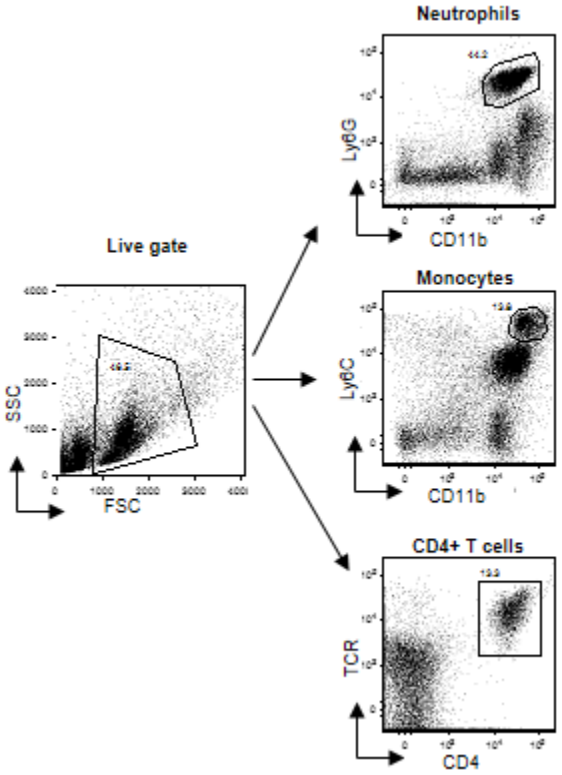

Supplementary figure 1. Gating strategy for analyzing specific immune cell subsets isolated from the CNS. Cells were isolated from the brain or spinal cord of mice with EAE and stained with antibodies specific for CD11b, Ly6G, Ly6C, TCR and CD4. Live cells were gated based on FSC and SSC. Neutrophils are within the $CD11b^{+}Ly6G^{+}$ gate, Monocytes are within the $CD11b^{+}Ly6C^{hi}$ gate, and $CD4^{+}$ T cells are within the $TCR^{+}CD4^{+}$ gate.

Chapter 8- Materials and Methods

Mice

C3HeB/FeJ mice were purchased from The Jackson Laboratory and bred and maintained in a specific pathogen-free facility at the University of Washington (Seattle, WA). IL-17RA$^{-/-}$ mice generated by Amgen were obtained from Taconic and backcrossed onto the C3HeB/FeJ mice for at least 12 generations. IFN-γR$^{-/-}$and GFAP-GFP transgenic mice were obtained from The Jackson Laboratory and backcrossed onto the C3HeB/FeJ background for at least 12 generations. Mice used for EAE induction were between 6 and 10 weeks of age. All procedures have been approved by the Institutional Animal Care and Use Committee at the University of Washington.

Protein and peptides

Recombinant rat MOG protein (rMOG; residues 1–125), was produced in *Escherichia coli* and purified as previously described [95]. $MOG_{97–114}$ peptide (rat sequence, TCFFRDHSYQEEAAVELK) was purchased from GenScript.

EAE induction

Passive EAE was induced by culturing splenocytes (1×10^7 cells/ml) from rMOG-immunized mice for 3 d with 5μg/ml $MOG_{97–114}$ peptide and 10 ng/ml rIL-23 (eBioscience). Viable cells were isolated from a lympholyte gradient (Cedarlane) and intraperitoneally injected (2×10^7 cells per mouse) into sublethally irradiated (250 rad) mice. Active EAE was induced as previously described [20]. Briefly, mice were immunized with 100ug rMOG in CFA, and injected with pertussis toxin on days 0 and 2 post-immunization. The severity of EAE was scored as follows (a grade was assigned when any one of its associated signs was observed): grade 1, paralyzed tail, hindlimb clasping; grade 2, head tilt, hindlimb weakness; grade 3, one paralyzed

leg, mild body leaning; grade 4, two paralyzed legs, moderate body leaning; grade 5, forelimb weakness, severe body leaning; grade 6, hunched, breathing difficulty, body rolling; grade 7, moribund. Atypical EAE was determined by the presence of one or more of the following symptoms: head tilt, body leaning, or body rolling.

Isolation of CNS cells

Mononuclear cells were isolated from the CNS of perfused EAE mice, as previously described [96]. Briefly, brain and spinal cord were dissociated with a 5-ml syringe plunger through a sterile stainless steel mesh and centrifuged for 10 min at 3000 rpm. Cell pellets were resuspended in 30% Percoll, overlaid onto 70% Percoll, and centrifuged without brake for 20 min at 2400 rpm. Cells were collected from the 30–70% Percoll interface.

For cell sorting experiments, cells were isolated from the CNS of perfused mice by digesting brains or spinal cords with 0.5mg/mL papain (Worthington Biochemical) and 20ng/ml DNase in HBSS for 20 minutes at 37ºC prior to isolating the cells on a Percoll gradient, in order to increase the number of viable astrocytes.

Flow cytometry

Cells were incubated with Fc block (clone 2.4G2; eBioscience) in normal mouse serum for 15 min at 4°C, washed, and stained with antibodies for 30 min at 4°C. Antibodies specific for CD4 (clone GK1.5), CD45 (clone 30-F11) and CD11b (M1/70) were from eBioscience . Antibodies specific for IFN-γ (clone XMG1.2), IL-17 (clone TC11-18H10), TCRβ (clone H57-597), Ly6G (clone 1A8), Ly6C (clone HK1.4), CD31 (clone MEC 13.3), and IFN-γRα (clone GR20) were from BD Biosciences. Cells were analyzed using a FACS Canto cytometer (BD Biosciences) and FlowJo software version 8.8.7 (Tree Star).

Quantitative RT-PCR

Tissue samples: Brain and spinal cord tissues were harvested from perfused naïve mice or mice with EAE (1-3 days post-onset, grade 3+) and snap-frozen in liquid nitrogen. Messenger RNA was extracted using RNeasy midi (brain tissue) or mini (spinal cord tissue) kits from Qiagen and first-strand cDNA was synthesized using SuperScript II (Invitrogen). Quantitative PCR was performed on an ABI 7300 Real Time PCR System (Applied Biosystems). Gene expression was normalized to values for *B-actin*.

Purified cells: cells were sorted from the brains and spinal cords separately of naïve mice and mice with EAE (1-3 days post-onset, grade 3+) using a FACS ARIA (BD Biosciences). Astrocytes were sorted from GFAP-GFP transgenic mice as $CD45^-$ GFP^+ cells and endothelial cells were sorted based on CD31 expression. Microglia and the subset of cells containing macrophages, monocyte and dendritic cells were sorted based on expression of CD45 and CD11b as previously described [97]. cDNA was generated using a *Power* SYBR® Green Cells-to-CT™ Kit (life technologies). Quantitative PCR was performed on an ABI ViiA 7 Real Time PCR System (Applied Biosystems). Gene expression was normalized to values for *GAPDH*.

In vivo treatments during EAE

The neutrophil-depleting antibody anti-Ly6G (clone 1A8) and isotype control antibody (clone 2A3) were purchased from Bio-X-Cell (West Lebanon, NH). Beginning on the day of T cell transfer, either 200 μg anti-Ly6G or isotype control (clone 2A3) was administered by intraperitoneal injection every other day until time of sacrifice (typically 7-8 days post-transfer). SB332235, the small molecule competitive antagonist of CXCR2 provided by GlaxoSmithKline (500 μg dissolved in 200 μL H_20), or vehicle control (H20) was administered to mice by oral gavage 2-3 times daily beginning on day of T cell transfer and continued until time of sacrifice

(typically 7-8 days post-transfer). The extent of neutrophil depletion in the blood was determined by complete blood count with differential, and the extent of neutrophil depletion in the spinal cord was assessed using flow cytometry. In the control spinal cord at peak EAE, >95% of $CD11b^{+}Ly6C^{mid}$ cells are neutrophils (verified by Ly6G staining). Therefore, neutrophils in the spinal cord of both control and anti-Ly6G-treated mice were identified as $CD11b^{+}Ly6C^{mid}$. However, $CD11b^{+}Ly6C^{mid}$ cells in the brain of control mice at peak EAE are comprised of both a $Ly6G^{+}$ and $Ly6G^{-}$ population and therefore was not a suitable gate for neutrophils.

Histochemical Analysis

Brains and spinal cords from mice with EAE were preserved in 10% neutral-buffered formalin, embedded in paraffin, sectioned and stained with hematoxylin and eosin. Sections were examined by a board-certified veterinary pathologist who was blinded to group assignments. The total sectional tissue area of multiple brain and cord sections from each mouse and the area of each focal, aggregated inflammatory/necrotic lesion within each section were measured using Nikon NIS-Elements software and expressed as percent of total brain or spinal cord. Numbers of vessels cuffed by inflammatory cells within each section were also counted and normalized to total tissue area. Included in the analysis was a semi-quantitative assessment of character and severity of tissue injury (manifested by necrotic and apoptotic cell death coupled with inflammatory cell accumulation graded on an inclusive scale of 1+ minimal to 4+ maximal injury).

Statistical analysis

Statistical analyses were performed with Prism version 5.0 (GraphPad Software), using an unpaired two-tailed Student *t* test or χ-square test. A p value <0.05 was considered significantly different.

References

1. International Multiple Sclerosis Genetics Consortium, et al., *Analysis of immune-related loci reveals 48 new susceptibility variants for multiple sclerosis.* Nat. Genet., 2013. **45**(11): p. 1353-60.
2. Noseworthy, J.H., et al., *Multiple sclerosis.* N Engl J Med, 2000. **343**(13): p. 938-52.
3. Lassmann, H., J. van Horssen, and D. Mahad, *Progressive multiple sclerosis: pathology and pathogenesis.* Nat Rev Neurol, 2012. **8**(11): p. 647-56.
4. Lucchinetti, C., et al., *Heterogeneity of multiple sclerosis lesions: implications for the pathogenesis of demyelination.* Annuals of Neurology, 2000. **47**(6): p. 707-717.
5. Giovannoni, G., *Management of secondary-progressive multiple sclerosis.* CNS Drugs, 2004. **18**(10): p. 653-69.
6. Weinshenker, B.G., et al., *The natural history of multiple sclerosis: a geographically based study. 2. Predictive value of the early clinical course.* Brain, 1989. **112 (Pt 6)**: p. 1419-28.
7. Thompson, A.J., et al., *Primary progressive multiple sclerosis.* Brain, 1997. **120 (Pt 6)**: p. 1085-96.
8. Lassmann, H., W. Bruck, and C.F. Lucchinetti, *The immunopathology of multiple sclerosis: an overview.* Brain Pathol, 2007. **17**(2): p. 210-8.
9. Vukusic, S. and C. Confavreux, *Primary and secondary progressive multiple sclerosis.* J Neurol Sci, 2003. **206**(2): p. 153-5.
10. Comi, G., *Disease-modifying treatments for progressive multiple sclerosis.* Mult Scler, 2013. **19**(11): p. 1428-36.
11. Nijeholt, G.J., et al., *Brain and spinal cord abnormalities in multiple sclerosis. Correlation between MRI parameters, clinical subtypes and symptoms.* Brain, 1998. **121 (Pt 4)**: p. 687-97.
12. Dutta, R. and B.D. Trapp, *Relapsing and progressive forms of multiple sclerosis: insights from pathology.* Curr Opin Neurol, 2014. **27**(3): p. 271-8.
13. Lassmann, H., *Hypoxia-like tissue injury as a component of multiple sclerosis lesions.* J Neurol Sci, 2003. **206**(2): p. 187-91.
14. Popescu, B.F. and C.F. Lucchinetti, *Pathology of demyelinating diseases.* Annu Rev Pathol, 2012. **7**: p. 185-217.
15. Thorpe, J.W., et al., *Spinal MRI in patients with suspected multiple sclerosis and negative brain MRI.* Brain, 1996. **119 (Pt 3)**: p. 709-14.
16. Nociti, V., et al., *Clinical characteristics, course and prognosis of spinal multiple sclerosis.* Spinal Cord, 2005. **43**(12): p. 731-4.
17. Kira, J., *Neuromyelitis optica and opticospinal multiple sclerosis: Mechanisms and pathogenesis.* Pathophysiology, 2011. **18**(1): p. 69-79.
18. Lennon, V.A., et al., *A serum autoantibody marker of neuromyelitis optica: distinction from multiple sclerosis.* Lancet, 2004. **364**(9451): p. 2106-12.
19. Stromnes, I.M. and J.M. Goverman, *Passive induction of experimental allergic encephalomyelitis.* Nature Protocols, 2006. **1**: p. 1952-1960.
20. Stromnes, I.M. and J.M. Goverman, *Active induction of experimental allergic encephalomyelitis.* Nature Protocols, 2006. **1**: p. 1810-1819.
21. McRae, B.L., et al., *Functional evidence for epitope spreading in the relapsing pathology of experimental autoimmune encephalomyelitis.* Journal of Experimental Medicine, 1995. **182**(1): p. 75-85.
22. McMahon, E.J., et al., *Epitope spreading initiates in the CNS in two mouse models of multiple sclerosis.* Nat Med, 2005. **11**(3): p. 335-9.

23. Tuohy, V.K., et al., *The epitope spreading cascade during progression of experimental autoimmune encephalomyelitis and multiple sclerosis.* Immunol Rev, 1998. **164**: p. 93-100.
24. Vanderlugt, C.L., et al., *The functional significance of epitope spreading and its regulation by co-stimulatory molecules.* Immunological Reviews, 1998. **164**: p. 63-72.
25. Vanderlugt, C.L., et al., *Pathologic role and temporal appearance of newly emerging autoepitopes in relapsing experimental autoimmune encephalomyelitis.* J Immunol, 2000. **164**(2): p. 670-8.
26. Katz-Levy, Y., et al., *Endogenous presentation of self myelin epitopes by CNS-resident APCs in Theiler's virus-infected mice.* J Clin Invest, 1999. **104**(5): p. 599-610.
27. Tompkins, S.M., K.G. Fuller, and S.D. Miller, *Theiler's virus-mediated autoimmunity: local presentation of CNS antigens and epitope spreading.* Ann N Y Acad Sci, 2002. **958**: p. 26-38.
28. Kroenke, M.A. and B.M. Segal, *Th17 and Th1 responses directed against the immunizing epitope, as opposed to secondary epitopes, dominate the autoimmune repertoire during relapses of experimental autoimmune encephalomyelitis.* J Neurosci Res, 2007. **85**(8): p. 1685-93.
29. Li, J., et al., *T cells that trigger acute experimental autoimmune encephalomyelitis also mediate subsequent disease relapses and predominantly produce IL-17.* J Neuroimmunol, 2011. **230**(1-2): p. 26-32.
30. Berard, J.L., et al., *Characterization of relapsing-remitting and chronic forms of experimental autoimmune encephalomyelitis in C57BL/6 mice.* Glia, 2010. **58**(4): p. 434-45.
31. Peiris, M., et al., *A model of experimental autoimmune encephalomyelitis (EAE) in C57BL/6 mice for the characterisation of intervention therapies.* J Neurosci Methods, 2007. **163**(2): p. 245-54.
32. Hampton, D.W., et al., *An experimental model of secondary progressive multiple sclerosis that shows regional variation in gliosis, remyelination, axonal and neuronal loss.* J Neuroimmunol, 2008. **201-202**: p. 200-11.
33. Basso, A.S., et al., *Reversal of axonal loss and disability in a mouse model of progressive multiple sclerosis.* J Clin Invest, 2008. **118**(4): p. 1532-43.
34. Al-Izki, S., et al., *Immunosuppression with FTY720 is insufficient to prevent secondary progressive neurodegeneration in experimental autoimmune encephalomyelitis.* Mult Scler, 2011. **17**(8): p. 939-48.
35. Pryce, G., et al., *Autoimmune tolerance eliminates relapses but fails to halt progression in a model of multiple sclerosis.* J Neuroimmunol, 2005. **165**(1-2): p. 41-52.
36. Farez, M.F., et al., *Toll-like receptor 2 and poly(ADP-ribose) polymerase 1 promote central nervous system neuroinflammation in progressive EAE.* Nat Immunol, 2009. **10**(9): p. 958-64.
37. Tsunoda, I., et al., *Massive apoptosis in lymphoid organs in animal models for primary and secondary progressive multiple sclerosis.* Am J Pathol, 2005. **167**(6): p. 1631-46.
38. Tsunoda, I., et al., *Converting relapsing remitting to secondary progressive experimental allergic encephalomyelitis (EAE) by ultraviolet B irradiation.* J Neuroimmunol, 2005. **160**(1-2): p. 122-34.
39. Serafini, B., et al., *Detection of ectopic B-cell follicles with germinal centers in the meninges of patients with secondary progressive multiple sclerosis.* Brain Pathol, 2004. **14**(2): p. 164-74.
40. Christopher Perrone, B.B., Peter Riskind and Carolina Ionete, *Abstract: A Two-Year Retrospective Analysis Of Rituximab Therapy In Secondary-Progressive Multiple Sclerosis* Neurology, 2014. **82**(10 Supplement P7.228).
41. Huseby, E.S., et al., *A pathogenic role for myelin-specific CD8(+) T cells in a model for multiple sclerosis.* Journal of Experimental Medicine, 2001. **194**(5): p. 669-676.
42. Komoly, S., *Experimental demyelination caused by primary oligodendrocyte dystrophy. Regional distribution of the lesions in the nervous system of mice [corrected].* Ideggyogy Sz, 2005. **58**(1-2): p. 40-3.

43. Liu, L., et al., *CXCR2-positive neutrophils are essential for cuprizone-induced demyelination: relevance to multiple sclerosis.* Nat Neurosci, 2010. **13**(3): p. 319-26.
44. Rodriguez, M., *Virus-induced demyelination in mice: "dying back" of oligodendrocytes.* Mayo Clin Proc, 1985. **60**(7): p. 433-8.
45. Endoh, M., et al., *DM-20, a proteolipid apoprotein, is an encephalitogen of acute and relapsing autoimmune encephalomyelitis in mice.* J Immunol, 1986. **137**(12): p. 3832-5.
46. Muller, D.M., M.P. Pender, and J.M. Greer, *A neuropathological analysis of experimental autoimmune encephalomyelitis with predominant brain stem and cerebellar involvement and differences between active and passive induction.* Acta Neuropathol (Berl), 2000. **100**(2): p. 174-82.
47. Baron, J.L., et al., *Surface expression of alpha 4 integrin by CD4 T cells is required for their entry into brain parenchyma.* Journal of Experimental Medicine, 1993. **177**(1): p. 57-68.
48. Segal, B.M. and E.M. Shevach, *IL-12 unmasks latent autoimmune disease in resistant mice.* J Exp Med, 1996. **184**(2): p. 771-5.
49. Merrill, J.E., et al., *Inflammatory leukocytes and cytokines in the peptide-induced disease of experimental allergic encephalomyelitis in SJL and B10.PL mice.* Proc Natl Acad Sci U S A, 1992. **89**(2): p. 574-8.
50. Renno, T., et al., *TNF-alpha expression by resident microglia and infiltrating leukocytes in the central nervous system of mice with experimental allergic encephalomyelitis. Regulation by Th1 cytokines.* J Immunol, 1995. **154**(2): p. 944-53.
51. Gran, B., et al., *IL-12p35-deficient mice are susceptible to experimental autoimmune encephalomyelitis: evidence for redundancy in the IL-12 system in the induction of central nervous system autoimmune demyelination.* J Immunol, 2002. **169**(12): p. 7104-10.
52. Becher, B., B.G. Durell, and R.J. Noelle, *Experimental autoimmune encephalitis and inflammation in the absence of interleukin-12.* J Clin Invest, 2002. **110**(4): p. 493-7.
53. Ferber, I.A., et al., *Mice with a disrupted IFN-gamma gene are susceptible to the induction of experimental autoimmune encephalomyelitis (EAE).* J Immunol, 1996. **156**(1): p. 5-7.
54. Hofstetter, H.H., et al., *Therapeutic efficacy of IL-17 neutralization in murine experimental autoimmune encephalomyelitis.* Cell Immunol, 2005. **237**(2): p. 123-30.
55. Komiyama, Y., et al., *IL-17 plays an important role in the development of experimental autoimmune encephalomyelitis.* Journal of Immunology, 2006. **177**(1): p. 566-73.
56. Gonzalez-Garcia, I., et al., *IL-17 signaling-independent central nervous system autoimmunity is negatively regulated by TGF-beta.* J Immunol, 2009. **182**(5): p. 2665-71.
57. Hu, Y., et al., *IL-17RC is required for IL-17A- and IL-17F-dependent signaling and the pathogenesis of experimental autoimmune encephalomyelitis.* J Immunol, 2010. **184**(8): p. 4307-16.
58. Kroenke, M.A., S.W. Chensue, and B.M. Segal, *EAE mediated by a non-IFN-gamma/non-IL-17 pathway.* Eur J Immunol, 2010. **40**(8): p. 2340-8.
59. Stromnes, I.M., et al., *Differential regulation of central nervous system autoimmunity by T(H)1 and T(H)17 cells.* Nat Med, 2008. **14**(3): p. 337-42.
60. Haak, S., et al., *IL-17A and IL-17F do not contribute vitally to autoimmune neuro-inflammation in mice.* J Clin Invest, 2009. **119**(1): p. 61-9.
61. Wensky, A.K., et al., *IFN-gamma determines distinct clinical outcomes in autoimmune encephalomyelitis.* J Immunol, 2005. **174**(3): p. 1416-23.
62. Lees, J.R., et al., *Regional CNS responses to IFN-gamma determine lesion localization patterns during EAE pathogenesis.* J Exp Med, 2008. **205**(11): p. 2633-42.
63. Lees, J.R., Y. Iwakura, and J.H. Russell, *Host T cells are the main producers of IL-17 within the central nervous system during initiation of experimental autoimmune encephalomyelitis induced by adoptive transfer of Th1 cell lines.* J Immunol, 2008. **180**(12): p. 8066-72.

64. Greer, J.M., et al., *Immunogenic and encephalitogenic epitope clusters of myelin proteolipid protein.* J Immunol, 1996. **156**(1): p. 371-9.
65. McRae, B.L., et al., *Induction of active and adoptive relapsing experimental autoimmune encephalomyelitis (EAE) using an encephalitogenic epitope of proteolipid protein.* Journal of Neuroimmunology, 1992. **38**(3): p. 229-240.
66. Pollinger, B., et al., *Spontaneous relapsing-remitting EAE in the SJL/J mouse: MOG-reactive transgenic T cells recruit endogenous MOG-specific B cells.* J Exp Med, 2009. **206**(6): p. 1303-16.
67. Bettelli, E., et al., *Myelin oligodendrocyte glycoprotein-specific T and B cells cooperate to induce a Devic-like disease in mice.* J Clin Invest, 2006. **116**(9): p. 2393-402.
68. Krishnamoorthy, G., et al., *Spontaneous opticospinal encephalomyelitis in a double-transgenic mouse model of autoimmune T cell/B cell cooperation.* J Clin Invest, 2006. **116**(9): p. 2385-92.
69. Abromson-Leeman, S., et al., *T-cell properties determine disease site, clinical presentation, and cellular pathology of experimental autoimmune encephalomyelitis.* Am J Pathol, 2004. **165**(5): p. 1519-33.
70. Liu, G.Y., et al., *Low avidity recognition of self-antigen by T cells permits escape from central tolerance.* Immunity, 1995. **3**(4): p. 407-415.
71. Gu, C., L. Wu, and X. Li, *IL-17 family: cytokines, receptors and signaling.* Cytokine, 2013. **64**(2): p. 477-85.
72. Gaffen, S.L., *Structure and signalling in the IL-17 receptor family.* Nat Rev Immunol, 2009. **9**(8): p. 556-67.
73. Ramana, C.V., et al., *Stat1-dependent and -independent pathways in IFN-gamma-dependent signaling.* Trends Immunol, 2002. **23**(2): p. 96-101.
74. Sadik, C.D., N.D. Kim, and A.D. Luster, *Neutrophils cascading their way to inflammation.* Trends Immunol, 2011. **32**(10): p. 452-60.
75. Carter, S.L., et al., *Induction of the genes for Cxcl9 and Cxcl10 is dependent on IFN-gamma but shows differential cellular expression in experimental autoimmune encephalomyelitis and by astrocytes and microglia in vitro.* Glia, 2007. **55**(16): p. 1728-39.
76. Huang, D., et al., *Chemokines and chemokine receptors in inflammation of the nervous system: manifold roles and exquisite regulation.* Immunol Rev, 2000. **177**: p. 52-67.
77. Gil, M.P., et al., *Biologic consequences of Stat1-independent IFN signaling.* Proc Natl Acad Sci U S A, 2001. **98**(12): p. 6680-5.
78. Prins, M., et al., *Interleukin-1beta and Interleukin-1 Receptor Antagonist Appear in Grey Matter Additionally to White Matter Lesions during Experimental Multiple Sclerosis.* PLoS One, 2013. **8**(12): p. e83835.
79. Li, X. and J.R. Lees, *Pre-existing central nervous system lesions negate cytokine requirements for regional experimental autoimmune encephalomyelitis development.* Immunology, 2013. **138**(3): p. 208-15.
80. Rothhammer, V., et al., *Th17 lymphocytes traffic to the central nervous system independently of alpha4 integrin expression during EAE.* J Exp Med, 2011. **208**(12): p. 2465-76.
81. Carlson, T., et al., *The Th17-ELR+ CXC chemokine pathway is essential for the development of central nervous system autoimmune disease.* J Exp Med, 2008. **205**(4): p. 811-23.
82. Tran, E.H., E.N. Prince, and T. Owens, *IFN-gamma shapes immune invasion of the central nervous system via regulation of chemokines.* J Immunol, 2000. **164**(5): p. 2759-68.
83. Kroenke, M.A. and B.M. Segal, *IL-23 modulated myelin-specific T cells induce EAE via an IFNgamma driven, IL-17 independent pathway.* Brain Behav Immun, 2011. **25**(5): p. 932-7.
84. McQualter, J.L., et al., *Granulocyte macrophage colony-stimulating factor: a new putative therapeutic target in multiple sclerosis.* J Exp Med, 2001. **194**(7): p. 873-82.

85. Ponomarev, E.D., et al., *GM-CSF production by autoreactive T cells is required for the activation of microglial cells and the onset of experimental autoimmune encephalomyelitis.* J Immunol, 2007. **178**(1): p. 39-48.
86. El-Behi, M., et al., *The encephalitogenicity of T(H)17 cells is dependent on IL-1- and IL-23-induced production of the cytokine GM-CSF.* Nat Immunol, 2011. **12**(6): p. 568-75.
87. Codarri, L., et al., *RORgammat drives production of the cytokine GM-CSF in helper T cells, which is essential for the effector phase of autoimmune neuroinflammation.* Nat Immunol, 2011. **12**(6): p. 560-7.
88. Lock, C., et al., *Gene-microarray analysis of multiple sclerosis lesions yields new targets validated in autoimmune encephalomyelitis.* Nature Medicine, 2002. **8**(5): p. 500-8.
89. Matusevicius, D., et al., *Interleukin-17 mRNA expression in blood and CSF mononuclear cells is augmented in multiple sclerosis.* Mult Scler, 1999. **5**(2): p. 101-4.
90. Bartosik-Psujek, H. and Z. Stelmasiak, *The levels of chemokines CXCL8, CCL2 and CCL5 in multiple sclerosis patients are linked to the activity of the disease.* Eur J Neurol, 2005. **12**(1): p. 49-54.
91. E. Havrdová, A.B., A. Goloborodko, A. Tisserant, I. Jones, H. Garren, D. Johns, *Late Breaking News 2: Positive proof of concept of AIN457, an antibody against interleukin-17A, in relapsing-remitting multiple sclerosis.* Multiple Sclerosis Journal, 2012. **18**(4 suppl): p. 513.
92. Chabas, D., et al., *Younger children with MS have a distinct CSF inflammatory profile at disease onset.* Neurology, 2010. **74**(5): p. 399-405.
93. Naegele, M., et al., *Neutrophils in multiple sclerosis are characterized by a primed phenotype.* J Neuroimmunol, 2012. **242**(1-2): p. 60-71.
94. Openshaw, H., et al., *Peripheral blood stem cell transplantation in multiple sclerosis with busulfan and cyclophosphamide conditioning: report of toxicity and immunological monitoring.* Biol Blood Marrow Transplant, 2000. **6**(5A): p. 563-75.
95. Abdul-Majid, K.B., et al., *Screening of several H-2 congenic mouse strains identified H-2(q) mice as highly susceptible to MOG-induced EAE with minimal adjuvant requirement.* J Neuroimmunol, 2000. **111**(1-2): p. 23-33.
96. Brabb, T., et al., *In situ tolerance within the central nervous system as a mechanism for preventing autoimmunity.* Journal of Experimental Medicine, 2000. **192**(6): p. 871-880.
97. Lee, S.Y. and J.M. Goverman, *The influence of T cell Ig mucin-3 signaling on central nervous system autoimmune disease is determined by the effector function of the pathogenic T cells.* J Immunol, 2013. **190**(10): p. 4991-9.